eliminated. However, given the limitation on restriction analysis, detecting small deletions on the EBV genome may be difficult. Since obtaining EBV mutants by PCR targeting does not involve a complex procedure, generating several mutants with the same mutation from independent experiments is relatively easy to achieve. Studying these mutants should yield results that reflect the functions of a mutated gene.

As is generally known, the expression of Rta and Zta is critical to the transcription of EBV lytic genes. This work demonstrates that many lytic genes are expressed at low levels by maxi-EBV under latent conditions (Fig. 2a and Supplementary Table S2), revealing that EBV lytic genes may be expressed in epithelial cells because of the constitutive expression of *BRLF1* in epithelial cells (Zalani *et al.*, 1992). On the other hand, lytic genes are no longer expressed after *BZLF1* and *BRLF1* are mutated (Fig. 2b, c; Supplementary Table S2), showing the importance of these two genes in activating the EBV lytic genes. Meanwhile, two spots containing the sequences of *BCRF2/EBNA-LP/BWRF1* (Fig. 2a and Supplementary Table S2, spot 2g) and *BYRF1* (EBNA2) (Fig. 2a and Supplementary Table S2, spot 2h) are transcribed at a higher level during latency (Fig. 2a and Supplementary Table S2). However, lytic induction reduces the transcription of these transcripts (Fig. 2d and Supplementary Table S2). Meanwhile, TPA and sodium butyrate treatment for 1 day increases the intensity of the EBER dot (Fig. 2d and Supplementary Table S2, spot 1h). These observations are inconsistent with what was observed in Akata cells, in which expression of *EBNA-LP* and *BYRF1* (EBNA2) increase and the expression of EBERs was unchanged after lytic induction by anti-IgG (Yuan *et al.*, 2006). Our results further demonstrate that a *BZLF1* mutation represses the expression of EBV genes; nearly no lytic gene is expressed by the mutant (Fig. 2b and Supplementary Table S2) and no virus particles are produced (Supplementary Fig. S1). Therefore, *BZLF1* is necessary to activate the viral lytic cycle. However, in this study, we also found that numbers of lytic genes are not fully expressed without Rta (Fig. 2f; Supplementary Table S2), and production of mature virion decreased by more than 90% (Supplementary Fig. S1); indicating that Rta is also crucial to EBV production. Thus, we conclude that without Rta, transcription of most EBV lytic genes is inefficient. Our recent study demonstrated that, rather than directly binding to Rta-response elements to activate transcription, Rta often interacts with MCAF1 to enhance Sp1-mediated transcription (Chang *et al.*, 2005). Rta also interacts with MCAF1 to enhance transcription mediated by transcription factors of the bZip family, including AP-1, ATF1/2 and Zta (L.-K. Chang & S.-T. Liu, unpublished results), implying that Rta often functions as a transcription co-activator to activate EBV lytic genes. The observations above may explain why EBV lytic genes are not fully expressed without Rta. Additionally, transcription of several crucial EBV lytic genes depends on Rta (Lu *et al.*, 2006), explaining why a mutation in *BRLF1* disrupts the EBV lytic cycle and why mutant MI-270 cannot generate EBV particles (Supplementary Fig. S1d). Moreover, according to our results, transfecting mutant MI-270 with pCMV-R does not enhance the transcription of *BcLF1* (VCA) (Fig. 2h and Supplementary Table S2, spots 9c, 9d, 9e, 9f), *BLLF1* (gp350/220) (Fig. 2h and Supplementary Table S2, spot 6e, 3f) and *BALF4* (gp110) (Fig. 2h and Supplementary Table S2, spots 11c, 11d). This analysis was performed using mRNA isolated from cells induced for the lytic cycle for 24 h. Accordingly, an extended lytic induction period may be necessary to observe how Rta affects the transcription of these genes. As is generally known, the behaviour of EBV in epithelial cells differs from that in B lymphocytes, which may explain why a recent work found that many lytic genes, including *BcLF1* (VCA), *BLLF1* (gp350/220) and *BALF4* (gp110), are fully expressed in Akata cells within 24 h of lytic induction by anti-IgG (Yuan *et al.*, 2006), indicating that cell types and the methods used for lytic induction may influence the timing of the transcription of lytic genes. Notably, several dots on the microarray chip used in this study may contain both latent and lytic genes (Supplementary Table S2). However, the dots that contain only EBV lytic genes are informative to the activation of EBV lytic genes by Rta and Zta.

The *BRLF1* promoter contains three ZREs. However, two studies that used transient transfection analysis yielded different results on the function of ZRE1 (Fig. 3a). Sinclair *et al.* (1991) found that mutating ZRE1 decreased the reporter activity by about 85%. However, Bhende *et al.* (2004) found that Zta preferentially binds to methylated ZRE2 and ZRE3 after lytic induction, and that ZRE1 plays small roles in the activation of *BRLF1* transcription. To further elucidate the functions of these ZREs in Rp, we mutated these sites on the EBV genome, and demonstrated that a ZRE1 mutation decreases *BRLF1* transcription by about 43% (Fig. 3g). This finding is inconsistent with the observation made by Bhende *et al.* (2004) and suggests that ZRE1 is important. This anomaly cannot be attributed to Rp methylation, as suggested by Bhende *et al.* (2004), since the Rp in maxi-EBV is hypermethylated in 293 cells (Bhende *et al.*, 2005); our own study also shows that nearly all the CpG sequences in the promoter are methylated during viral latency. Furthermore, an upstream region in the *BRLF1* promoter between positions −965 and −852 is crucial to the activation by Zta; without this fragment, the promoter cannot be fully activated by pCMV-Z (Fig. 3c, R-850). These experiments also demonstrate the feasibility of generating site-specific mutations in a promoter on the EBV genome to analyse the promoter function.

This work demonstrates that a mutation in *BDLF1* and *BORF1* yields strains that cannot assemble EBV capsids in the cell (Fig. 4c) or yield viral particles (Fig. 4a). Additionally, BDLF1 and BORF1 proteins are 17.7 and 19% homologous with UL18 and UL38 proteins, two minor capsid proteins from HSV-1, indicating that BDLF1 and BORF1 proteins are components of the EBV capsid.

Furthermore, this study finds that transfecting a plasmid that overexpresses the two minor capsid proteins into the mutant strains cannot genetically complement the mutations (Fig. 4e). This result is not completely surprising because our recent work revealed that the BDLF1 and BORF1 proteins interact not only with each other but also with VCA (W.-H. Wang & S.-T. Liu, unpublished results). Therefore, when one of the two minor capsid proteins becomes more abundant in the cells, the interaction between overexpressed proteins and VCA or the other minor capsid protein is preferred and the formation of a complex that contains VCA, BORF1 and BDLF1 proteins is actually prevented. This investigation also reveals an intrinsic problem of the techniques adopted herein: revertants are difficult to obtain to verify the mutational effects. Therefore, mutant strains which contain the same mutation, generated from independent experiments, must be investigated to confirm the experimental results. This study demonstrates the usefulness of a comprehensive library of EBV mutants, likely to be invaluable in EBV research.

ACKNOWLEDGEMENTS

We would like to thank Bill Sugden for his criticisms and suggestions, Mei Chao for providing the anti-EBNA1 antibody, as well as Barry Wanner and Nicholas Bird for the plasmids for PCR targeting. This research is supported by National Science Council of the Republic of China, Taiwan (NSC96-3112-B-182-002), National Health Research Institute of the Republic of China (NHRI-EX96-9417BI) and Chang-Gung Molecular Medicine Research Center (CMRPD160111).

REFERENCES

Ahsan, N., Kanda, T., Nagashima, K. & Takada, K. (2005). Epstein-Barr virus transforming protein LMP1 plays a critical role in virus production. *J Virol* **79**, 4415–4424.

Altmann, M., Pich, D., Ruiss, R., Wang, J., Sugden, B. & Hammerschmidt, W. (2006). Transcriptional activation by EBV nuclear antigen 1 is essential for the expression of EBV's transforming genes. *Proc Natl Acad Sci U S A* **103**, 14188–14193.

Asai, R., Kato, A., Kato, K., Kanamori-Koyama, M., Sugimoto, K., Sairenji, T., Nishiyama, Y. & Kawaguchi, Y. (2006). Epstein-Barr virus protein kinase BGLF4 is a virion tegument protein that dissociates from virions in a phosphorylation-dependent process and phosphorylates the viral immediate-early protein BZLF1. *J Virol* **80**, 5125–5134.

Bhende, P. M., Seaman, W. T., Delecluse, H. J. & Kenney, S. C. (2004). The EBV lytic switch protein, Z, preferentially binds to and activates the methylated viral genome. *Nat Genet* **36**, 1099–1104.

Bhende, P. M., Seaman, W. T., Delecluse, H. J. & Kenney, S. C. (2005). BZLF1 activation of the methylated form of the BRLF1 immediate-early promoter is regulated by BZLF1 residue 186. *J Virol* **79**, 7338–7348.

Bloss, T. A. & Sugden, B. (1994). Optimal lengths for DNAs encapsidated by Epstein-Barr virus. *J Virol* **68**, 8217–8222.

Chang, L. K. & Liu, S. T. (2000). Activation of the BRLF1 promoter and lytic cycle of Epstein–Barr virus by histone acetylation. *Nucleic Acids Res* **28**, 3918–3925.

Chang, L. K., Wei, T. T., Chiu, Y. F., Tung, C. P., Chuang, J. Y., Hung, S. K., Li, C. & Liu, S. T. (2003). Inhibition of Epstein–Barr virus lytic cycle by (−)-epigallocatechin gallate. *Biochem Biophys Res Commun* **301**, 1062–1068.

Chang, L. K., Chung, J. Y., Hong, Y. R., Ichimura, T., Nakao, M. & Liu, S. T. (2005). Activation of Sp1-mediated transcription by Rta of Epstein–Barr virus via an interaction with MCAF1. *Nucleic Acids Res* **33**, 6528–6539.

Chau, C. M., Zhang, X. Y., McMahon, S. B. & Lieberman, P. M. (2006). Regulation of Epstein-Barr virus latency type by the chromatin boundary factor CTCF. *J Virol* **80**, 5723–5732.

Chen, A., Divisconte, M., Jiang, X., Quink, C. & Wang, F. (2005). Epstein-Barr virus with the latent infection nuclear antigen 3B completely deleted is still competent for B-cell growth transformation in vitro. *J Virol* **79**, 4506–4509.

Collins, C. M., Medveczky, M. M., Lund, T. & Medveczky, P. G. (2002). The terminal repeats and latency-associated nuclear antigen of herpesvirus saimiri are essential for episomal persistence of the viral genome. *J Gen Virol* **83**, 2269–2278.

Datsenko, K. A. & Wanner, B. L. (2000). One-step inactivation of chromosomal genes in *Escherichia coli* K-12 using PCR products. *Proc Natl Acad Sci U S A* **97**, 6640–6645.

Decaussin, G., Leclerc, V. & Ooka, T. (1995). The lytic cycle of Epstein-Barr virus in the nonproducer Raji line can be rescued by the expression of a 135-kilodalton protein encoded by the BALF2 open reading frame. *J Virol* **69**, 7309–7314.

Delecluse, H. J., Hilsendegen, T., Pich, D., Zeidler, R. & Hammerschmidt, W. (1998). Propagation and recovery of intact, infectious Epstein-Barr virus from prokaryotic to human cells. *Proc Natl Acad Sci U S A* **95**, 8245–8250.

Delecluse, H. J., Pich, D., Hilsendegen, T., Baum, C. & Hammerschmidt, W. (1999). A first-generation packaging cell line for Epstein-Barr virus-derived vectors. *Proc Natl Acad Sci U S A* **96**, 5188–5193.

Dirmeier, U., Neuhierl, B., Kilger, E., Reisbach, G., Sandberg, M. L. & Hammerschmidt, W. (2003). Latent membrane protein 1 is critical for efficient growth transformation of human B cells by Epstein-Barr virus. *Cancer Res* **63**, 2982–2989.

Farina, A., Feederle, R., Raffa, S., Gonnella, R., Santarelli, R., Frati, L., Angeloni, A., Torrisi, M. R., Faggioni, A. & Delecluse, H. J. (2005). BFRF1 of Epstein-Barr virus is essential for efficient primary viral envelopment and egress. *J Virol* **79**, 3703–3712.

Feederle, R. & Delecluse, H. J. (2004). Low level of lytic replication in a recombinant Epstein-Barr virus carrying an origin of replication devoid of BZLF1-binding sites. *J Virol* **78**, 12082–12084.

Feederle, R., Kost, M., Baumann, M., Janz, A., Drouet, E., Hammerschmidt, W. & Delecluse, H. J. (2000). The Epstein–Barr virus lytic program is controlled by the co-operative functions of two transactivators. *EMBO J* **19**, 3080–3089.

Feederle, R., Shannon-Lowe, C., Baldwin, G. & Delecluse, H. J. (2005). Defective infectious particles and rare packaged genomes produced by cells carrying terminal-repeat-negative Epstein-Barr virus. *J Virol* **79**, 7641–7647.

Feederle, R., Neuhierl, B., Baldwin, G., Bannert, H., Hub, B., Mautner, J., Behrends, U. & Delecluse, H. J. (2006). Epstein-Barr virus BNRF1 protein allows efficient transfer from the endosomal compartment to the nucleus of primary B lymphocytes. *J Virol* **80**, 9435–9443.

Grabusic, K., Maier, S., Hartmann, A., Mantik, A., Hammerschmidt, W. & Kempkes, B. (2006). The CR4 region of EBNA2 confers viability of Epstein–Barr virus-transformed B cells by CBF1-independent signalling. *J Gen Virol* **87**, 3169–3176.

Griffin, B. E., Bjorck, E., Bjursell, G. & Lindahl, T. (1981). Sequence complexity of circular Epstein-Bar virus DNA in transformed cells. *J Virol* **40**, 11–19.

Gust, B., Challis, G. L., Fowler, K., Kieser, T. & Chater, K. F. (2003). PCR-targeted *Streptomyces* gene replacement identifies a protein domain needed for biosynthesis of the sesquiterpene soil odor geosmin. *Proc Natl Acad Sci U S A* **100**, 1541–1546.

Hatfull, G., Bankier, A. T., Barrell, B. G. & Farrell, P. J. (1988). Sequence analysis of Raji Epstein-Barr virus DNA. *Virology* **164**, 334–340.

Ho, S. N., Hunt, H. D., Horton, R. M., Pullen, J. K. & Pease, L. R. (1989). Site-directed mutagenesis by overlap extension using the polymerase chain reaction. *Gene* **77**, 51–59.

Hong, G. K., Delecluse, H. J., Gruffat, H., Morrison, T. E., Feng, W. H., Sergeant, A. & Kenney, S. C. (2004). The BRRF1 early gene of Epstein-Barr virus encodes a transcription factor that enhances induction of lytic infection by BRLF1. *J Virol* **78**, 4983–4992.

Humme, S., Reisbach, G., Feederle, R., Delecluse, H. J., Bousset, K., Hammerschmidt, W. & Schepers, A. (2003). The EBV nuclear antigen 1 (EBNA1) enhances B cell immortalization several thousandfold. *Proc Natl Acad Sci U S A* **100**, 10989–10994.

Hung, C. H. & Liu, S. T. (1999). Characterization of the Epstein–Barr virus BALF2 promoter. *J Gen Virol* **80**, 2747–2750.

Hutchings, I. A., Tierney, R. J., Kelly, G. L., Stylianou, J., Rickinson, A. B. & Bell, A. I. (2006). Methylation status of the Epstein-Barr virus (EBV) *Bam*HI W latent cycle promoter and promoter activity: analysis with novel EBV-positive Burkitt and lymphoblastoid cell lines. *J Virol* **80**, 10700–10711.

Janz, A., Oezel, M., Kurzeder, C., Mautner, J., Pich, D., Kost, M., Hammerschmidt, W. & Delecluse, H. J. (2000). Infectious Epstein-Barr virus lacking major glycoprotein BLLF1 (gp350/220) demonstrates the existence of additional viral ligands. *J Virol* **74**, 10142–10152.

Kado, C. I. & Liu, S. T. (1981). Rapid procedure for detection and isolation of large and small plasmids. *J Bacteriol* **145**, 1365–1373.

Kanda, T., Yajima, M., Ahsan, N., Tanaka, M. & Takada, K. (2004). Production of high-titer Epstein-Barr virus recombinants derived from Akata cells by using a bacterial artificial chromosome system. *J Virol* **78**, 7004–7015.

Kelly, G. L., Milner, A. E., Tierney, R. J., Croom-Carter, D. S., Altmann, M., Hammerschmidt, W., Bell, A. I. & Rickinson, A. B. (2005). Epstein-Barr virus nuclear antigen 2 (EBNA2) gene deletion is consistently linked with EBNA3A, -3B, and -3C expression in Burkitt's lymphoma cells and with increased resistance to apoptosis. *J Virol* **79**, 10709–10717.

Li, C., Chen, R. S., Hung, S. K., Lee, Y. T., Yen, C. Y., Lai, Y. W., Teng, R. H., Huang, J. Y., Tang, Y. C. & other authors (2006). Detection of Epstein–Barr virus infection and gene expression in human tumors by microarray analysis. *J Virol Methods* **133**, 158–166.

Lu, C. C., Jeng, Y. Y., Tsai, C. H., Liu, M. Y., Yeh, S. W., Hsu, T. Y. & Chen, M. R. (2006). Genome-wide transcription program and expression of the Rta responsive gene of Epstein-Barr virus. *Virology* **345**, 358–372.

Murphy, K. C. (1998). Use of bacteriophage lambda recombination functions to promote gene replacement in *Escherichia coli*. *J Bacteriol* **180**, 2063–2071.

Neuhierl, B. & Delecluse, H. J. (2006). The Epstein-Barr virus BMRF1 gene is essential for lytic virus replication. *J Virol* **80**, 5078–5081.

Ryan, J. L., Fan, H., Glaser, S. L., Schichman, S. A., Raab-Traub, N. & Gulley, M. L. (2004). Epstein-Barr virus quantitation by real-time PCR targeting multiple gene segments: a novel approach to screen for the virus in paraffin-embedded tissue and plasma. *J Mol Diagn* **6**, 378–385.

Sambrook, J., Fritsch, E. F. & Maniatis, T. (1989). *Molecular Cloning: A Laboratory Manual.* Cold Spring Harbor, NY: Cold Spring Harbor Laboratory.

Shannon-Lowe, C. D., Neuhierl, B., Baldwin, G., Rickinson, A. B. & Delecluse, H. J. (2006). Resting B cells as a transfer vehicle for Epstein-Barr virus infection of epithelial cells. *Proc Natl Acad Sci U S A* **103**, 7065–7070.

Sharma, R. C. & Schimke, R. T. (1996). Preparation of electro-competent *E. coli* using salt-free growth medium. *Biotechniques* **20**, 42–44.

Sinclair, A. J., Brimmell, M., Shanahan, F. & Farrell, P. J. (1991). Pathways of activation of the Epstein-Barr virus productive cycle. *J Virol* **65**, 2237–2244.

Skare, J., Farley, J., Strominger, J. L., Fresen, K. O., Cho, M. S. & zur Hausen, H. (1985). Transformation by Epstein-Barr virus requires DNA sequences in the region of *Bam*HI fragments Y and H. *J Virol* **55**, 286–297.

Song, M. J., Hwang, S., Wong, W. H., Wu, T. T., Lee, S., Liao, H. I. & Sun, R. (2005). Identification of viral genes essential for replication of murine gamma-herpesvirus 68 using signature-tagged mutagenesis. *Proc Natl Acad Sci U S A* **102**, 3805–3810.

Wang, X. & Hutt-Fletcher, L. M. (1998). Epstein-Barr virus lacking glycoprotein gp42 can bind to B cells but is not able to infect. *J Virol* **72**, 158–163.

Wang, J. T., Yang, P. W., Lee, C. P., Han, C. H., Tsai, C. H. & Chen, M. R. (2005). Detection of Epstein–Barr virus BGLF4 protein kinase in virus replication compartments and virus particles. *J Gen Virol* **86**, 3215–3225.

Yuan, J., Cahir-McFarland, E., Zhao, B. & Kieff, E. (2006). Virus and cell RNAs expressed during Epstein-Barr virus replication. *J Virol* **80**, 2548–2565.

Zalani, S., Holley-Guthrie, E. A., Gutsch, D. E. & Kenney, S. C. (1992). The Epstein-Barr virus immediate-early promoter BRLF1 can be activated by the cellular Sp1 transcription factor. *J Virol* **66**, 7282–7292.

Microbiol. Immunol., **51**(6), 609–616, 2007

Duration of Neutralizing Antibody Titer after Japanese Encephalitis Vaccination

Motoharu Abe*[,1], Kenji Okada[2], Kenshi Hayashida[1], Fujio Matsuo[1], Kouichi Shiosaki[1], Chiaki Miyazaki[3], Kohji Ueda[4], and Yoichiro Kino[1]

[1]The Chemo-Sero-Therapeutic Research Institute, Kikuchi Research Center, Kikuchi, Kumamoto 869–1298, Japan, [2]Division of Pediatrics, National Hospital Organization Fukuoka National Hospital, Fukuoka, Fukuoka 811–1394, Japan, [3]Fukuoka-West Rehabilitation Center for Children, Fukuoka, Fukuoka 819–0005, Japan, and [4]Faculty of Health and Welfare, Seinan Jo Gakuin University, Kitakyushu, Fukuoka 803–0835, Japan

Received December 8, 2006; in revised form, March 7, 2007. Accepted March 9, 2007

***Abstract*: In paired serum samples collected from 17 children, we measured neutralizing antibody (NTAb) titers after the second series of routine Japanese encephalitis (JE) vaccination in Japan to estimate the duration of NTAb titer when children did not receive the third series of routine vaccination by applying a random coefficient model. We also measured NTAb titers in adult serum samples to confirm the duration of NTAb titer estimated in the analysis of pediatric serum samples. In the absence of the third series of routine vaccination, 18% (3/17), 47% (8/17), 82% (14/17) and 100% (17/17) of children were estimated to become NTAb negative at 5, 10, 15, and 20 years after the second series of routine vaccination, respectively. Of 38 adults, 39.5% (15/38) became NTAb negative; the percentage was somewhat lower than that of antibody-negative children. The results suggested that JE vaccination schedule should be reevaluated in the future.**

***Key words*: Japanese encephalitis vaccine, Japanese encephalitis virus, Routine vaccination in Japan, Duration of neutralizing antibody titer**

Japanese encephalitis (JE), or Japanese encephalitis virus (JEV) infection, is an endemic disease in Japan as well as in the other Asian countries. Approximately 50,000 JE patients are reported annually, mainly in Southeast Asia (29). The JE endemic area has been expanding (13–15, 29). JE is an inflammatory disease that affects the central nervous system. Sudden fever, headache, and vomiting occur after 7 to 10 days incubation period. Approximately 30% of JE cases end fatally, and 50% of patients are left with neurological sequelae (9).

The mouse brain-derived JE vaccine was first approved in 1954, and the vaccine strain was switched from the Nakayama strain to the Beijing-1 strain in 1988 in order to enhance the vaccination effectiveness (23), resulting in a dramatic decrease of JE patients. Although only a small number of JE patients have been reported annually in Japan in recent years, the infection rate remains high in swine which is an intermediate host of JEV (6, 9). Human vaccination and JEV antibody surveillance are therefore essential tools from the public health point of view (10). If there are neutralizing antibody (NTAb) titers of 1:10 or more, it is thought that natural infection of a JEV can be prevented (2, 8, 16, 19, 29). Moreover, the World Health Organization (WHO) described in its 2006 position paper that NTAb titers of 1:10 or more were accepted evidence of protection against JEV infection (27).

As shown in Fig. 1, JE vaccination had been provided in the three-series routine vaccination program in Japan (9, 23).

However, the Ministry of Health, Labour and Welfare (MHLW) of Japan decided in May 2005 to suspend its recommendation of the routine vaccination with the current mouse brain-derived vaccine until a safer JE vaccine was available because of associated adverse effects including acute disseminated encephalomyelitis (18, 28). In July 2005, MHLW announced that the third series of vaccination would not be resumed even

**Address correspondence to* Dr. Motoharu Abe, The Chemo-Sero-Therapeutic Research Institute, Kikuchi Research Center, Kikuchi, Kumamoto 869–1298, Japan. Fax: +81–968–37–4350. E-mail: abe-mo@kaketsuken.or.jp

Abbreviations: 3LSRM, 3 points least-squares regression method; CI, confidence interval; GMT, geometric mean titer; JE, Japanese encephalitis; JEV, Japanese encephalitis virus; MHLW, Ministry of Health, Labour and Welfare; NTAb, neutralizing antibody.

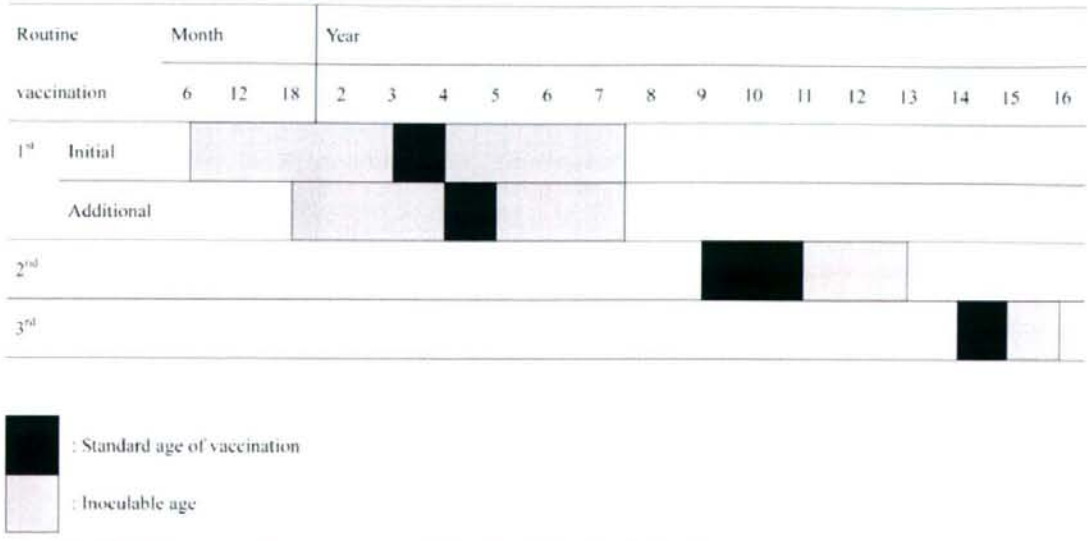

Fig. 1. In Japan, a JE routine vaccination was generally performed as follows: the first series of routine vaccinations is performed twice at 1 to 4 weeks interval between 6 to 90 months old (standard age is 3 years old) as initial vaccinations and one more time about 1 year after initial vaccinations (standard age is 4 years old) as an additional vaccination; the second series of routine vaccination is performed between 9 and 12 years old (standard age is 9 to 10 years old); the third series of routine vaccination is performed between 14 and 15 years old (standard age is 14 years old).

after a safer vaccine became available.

However, 4 of 57 cerebrospinal fluid samples collected from patients with undiagnosed acute encephalomeningitis were tested JEV genome positive (11), suggesting that the etiology of JEV infection has changed. In 2006, 7 JE patients, including a 3-year-old, were identified in Japan. Many Japanese travel to Southeast Asia where JEV infection is a big concern (3, 21). Considering these facts, maintaining sufficient NTAb to prevent JEV infection is still important for people of all ages in present-day Japan. We are currently developing a Vero cell-derived vaccine to replace the mouse brain-derived vaccine in order to improve vaccine safety and productivity (2, 7, 12, 22). However, little information is available concerning NTAb prevalence based on the JE vaccination schedule shown in Fig. 1 (6). Reviewing the JE vaccination schedule before introducing a Vero cell-derived vaccine will therefore be meaningful.

In the current study, we measured NTAb titers in pediatric serum samples including paired serum samples to estimate the duration of NTAb titer after the current routine JE vaccination program by applying a random coefficient model. We also measured adult serum NTAb titers to support the estimated duration of NTAb titer based on the analysis of pediatric serum samples.

Materials and Methods

Pediatric serum samples after completion of the second series of routine vaccination. Serum samples were collected from 47 children who lived in Hisayama-machi, Fukuoka prefecture, Japan, a potential JE high-risk area based on the prevalence of antibodies against JEV in swine (6, 9), and had completed the second series of routine JE vaccination. The sample collection took place in 1994 and 1997 after obtaining informed consent of the participants to provide their serum samples for measurement of antibodies against infectious diseases. The history of JE vaccination was checked by referring to the mother-child notebook of each participant. The collected samples included paired serum samples (collected in 1994 and 1997) of 17 participants and single serum samples (collected in 1997) of 30 participants. The first samples of paired serum were collected about 2 months after the second series of vaccination in 1994. The second samples of paired serum were collected about 38 months after the second series and before the third series of vaccination in 1997. Each of the single serum samples collected in 1997 consisted of those collected about 2 months after ($n=12$) or about 38 months after ($n=18$) the second series of vaccination. All serum samples were stored at −80 C until

NTAb titers were measured.

Adult serum samples. Thirty-eight adult serum samples were used to determine the accuracy of duration of NTAb estimated in the analysis of pediatric serum samples. All the adult serum samples were collected from visitors at the outpatient vaccination department of the National Hospital Organization Fukuoka National Hospital living in Fukuoka prefecture, Japan, and scheduled to travel to Southeast Asia. Informed consent to provide the serum sample for measurement of NTAbs against JEV was obtained from the visitors. Their ages ranged from 24 to 55, and their history of vaccination was unknown. Most visitors wished to receive an additional JE vaccination prior to their departure. Serum samples were obtained from 18 visitors at least 3 weeks after the additional vaccination. All serum samples were stored at −80 C until NTAb titers were measured.

Neutralizing antibody titer assay. Fifty-percent plaque reduction test with Vero cells was used to measure NTAbs in the serum samples, and 3 points least-squares regression method (3LSRM) described in our previous study was used for analysis (1). The standard deviation in 3LSRM is 0.127 (log) or less and the variation coefficient is 7% or less (1).

Statistical analysis. Geometric mean, standard deviation, and range of NTAb titers after the second series of routine vaccination were separately calculated for the paired serum samples and the single serum samples. For the paired serum samples, the geometric mean titer (GMT) ratio of NTAb titers at about 38 months after the second series of routine vaccination against those at about 2 months after and 95% confidence interval (CI) were calculated. A random coefficient model was applied to the NTAb titers in the paired and single serum samples in order to estimate time when the NTAbs acquired by JE vaccination turned negative (less than 1:10).

$$y_{ij}=\alpha+\beta x_i+a^*_i+b^*_i x_{ij}+\varepsilon_{ij} \qquad \text{(I)}$$

where

$i=1, \ldots, t$

$j=1, \ldots, n_i$

$a^*_i=a_i-\alpha$

$b^*_i=b_i-\beta$

$$\begin{pmatrix} a^*_i \\ b^*_i \end{pmatrix} \sim iidN\left[\begin{pmatrix} 0 \\ 0 \end{pmatrix}, \psi\right], \quad \psi=\begin{pmatrix} \sigma^2_a & \sigma_{ab} \\ \sigma_{ab} & \sigma^2_b \end{pmatrix}$$

$\varepsilon_{ij} \sim iidN(0, \sigma^2)$

y_{ij} in Equation (I) represents the NTAbs in participant i ($1, \ldots, t$) at measuring timepoint j ($1, \ldots, n_i$) after logarithmic conversion. α represents the intercept of the entire population, x_i represents the number of years after the last vaccination, β represents the slope of changes in NTAbs in the entire population, a^*_i represents the difference between the intercept of participant i and that of the entire population, b^*_i represents the difference between the slope of participant i and that of the entire population, and ε_{ij} represents the residual error. $\alpha+\beta x_i$ represents the fixed effect of the model (population mean), and $a^*_i+b^*_i x_{ij}+\varepsilon_{ij}$ represents the deviation from the fixed effect of the model, or the random (intra-participant) effect. Random effects a^*_i and b^*_i were independent and identically distributed (mean (0, 0), variance ψ) and so did residual error ε_{ij} (mean 0, variance σ^2). SAS (SAS Institute, Cary, N.C., U.S.A.) was used for all statistical analyses.

Results

Neutralizing Antibody Titers in Paired and Single Serum Samples

Distribution of NTAb titers in paired and single serum samples collected after the second series of routine JE vaccination is shown in Fig. 2.

Geometric mean of NTAb titers in paired serum samples of 17 fourth graders (aged 9 to 10) at approximately 2 months after the vaccination was $1:10^{2.876}$ (standard deviation, $1:10^{0.737}$; minimum, $1:10^{1.57}$; maximum, $1:10^{3.95}$). When the children became seventh graders (aged 12 to 13) approximately 3 years after the initial analysis, the geometric mean of NTAb titers significantly decreased to $1:10^{2.303}$ (standard deviation, $1:10^{0.826}$; minimum, $1:10^{0.90}$; maximum, $1:10^{3.50}$; GMT ratio, 0.267; two-sided 95% CI, 0.076 to 0.940). All individual paired serum samples showed a flat decrease in NTAb titers; however, there were inter-individual differences in the slope of decrease (range of individual regression coefficient, −0.11 to −1.42) (Fig. 2).

The geometric mean of NTAb titers in single serum samples of 12 children collected only at 2 months after the vaccination was $1:10^{3.693}$ (standard deviation, $1:10^{0.290}$; minimum, $1:10^{3.06}$; maximum, $1:10^{4.10}$) and in serum samples of 18 children collected only at 38 months after the vaccination, it was $1:10^{2.266}$ (standard deviation, $1:10^{0.864}$; minimum, $1:10^{0.97}$; maximum, $1:10^{3.45}$). Neutralizing antibody titers in many of the single serum samples collected at 2 months post-vaccination were higher compared with the paired serum samples collected around the same time. On the other hand, NTAb titers in the single serum samples collected at 38 months post-vaccination were comparable to those in the paired serum samples collected around the same time (Fig. 2).

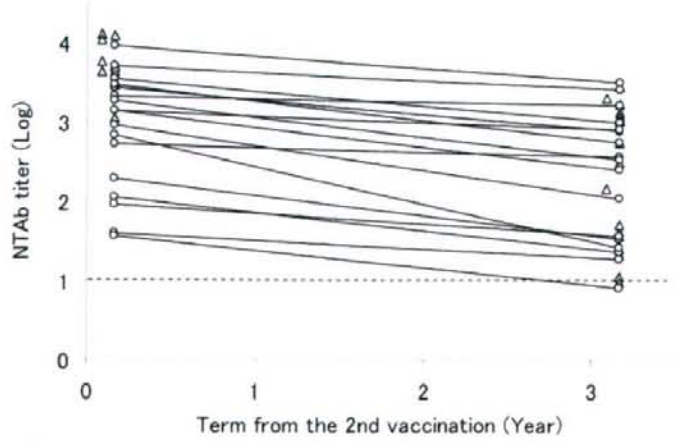

Fig. 2. Neutralizing antibody titers in paired pediatric serum samples: ○ ($n=17$) and single pediatric serum samples: △ ($n=30$) after second series of routine Japanese encephalitis vaccination.

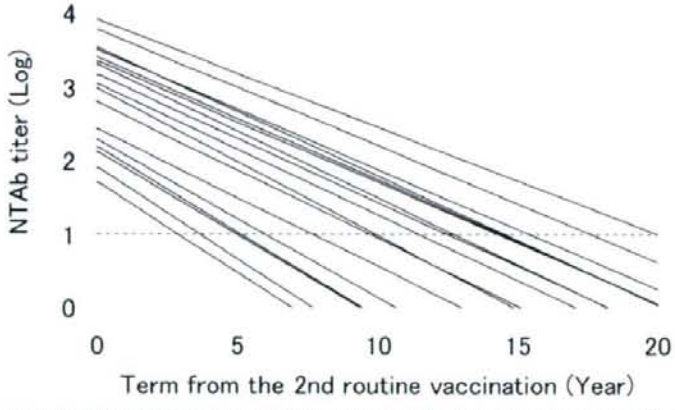

Fig. 3. Estimated individual NTAb titers in pediatric serum samples based on random coefficient model ($n=17$).

Duration of Neutralizing Antibody Titer after the Second Series of Routine Vaccination

A random coefficient model was applied to the NTAb titers in the paired serum samples collected from 17 children in order to estimate the time until the NTAbs acquired through JE vaccination turned negative (less than 1:10) in individual children (Fig. 3).

At 5, 10, 15, and 20 years after vaccination, 18% (3/17), 47% (8/17), 82% (14/17) and 100% (17/17) of the children, respectively, were estimated to become NTAb negative. Time to negative NTAb titers was also estimated for sensitivity analysis by using single serum samples collected from 30 children (samples of 12 children collected at 2 months post-vaccination and those of 18 children collected at 38 months post-vaccination) in addition to the said paired serum samples of 17 children (47 samples in total, Fig. 4).

At 5, 10, 15, and 20 years post-vaccination, 15% (7/47), 38% (18/47), 70% (33/47) and 89% (42/47) of children, respectively, were estimated to become NTAb negative. The results were comparable to those estimated by using the paired serum samples of only 17 children. However, the estimates of the 17 paired serum samples calculated by each population were different (Figs. 3 and 4).

Adult Serum Samples

Neutralizing antibody titers in 38 adults aged between 24 and 55 are shown in Fig. 5.

Negative NTAb titers were found in 39.5% (15/38)

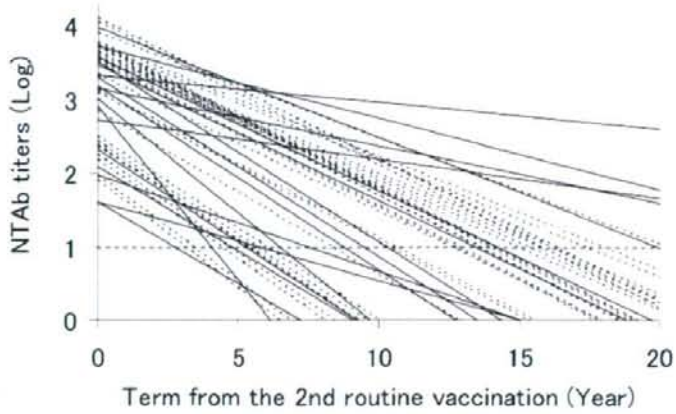

Fig. 4. Estimated individual NTAb titers in pediatric serum samples based on random coefficient model (n=47). The solid lines indicate paired pediatric serum samples (n=17) and the broken lines indicate single pediatric serum samples (n=30).

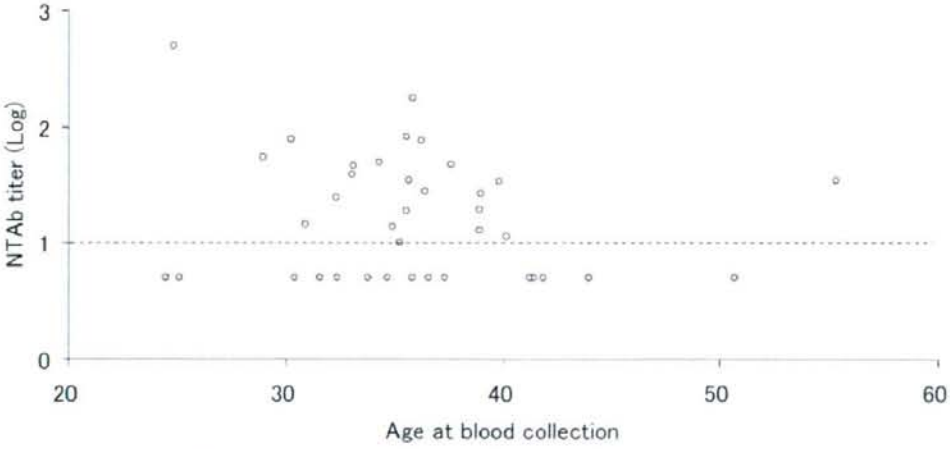

Fig. 5. Distribution of NTAb titers in adult serum samples (n=38). Neutralizing antibody titer in a NTAb negative sample is shown as 0.7.

and NTAb titers of $1:10^{1.5}$ or less were found in 65.8% (25/38). Only 2 adults had NTAb titers of $1:10^{2.0}$ or more. In the age-specific analysis, 50.0% (2/4) of those under 30, 29.6% (8/27) of those aged 30 or above and under 40, and 71.4% (5/7) of those aged 40 or above had negative NTAb titers. A higher negative rate was seen in adults aged 40 or above. After additional vaccination, serum samples were collected for further analysis from 18 adults as shown in Fig. 6. All of the 8 volunteers who had had negative NTAb titers had positive NTAb titers.

Discussion

With the revision of the Preventive Vaccination Law in 1994, the JE vaccination program was changed from mass vaccination to individual vaccination in Japan. The JE vaccination rate among children, especially those of the second and third series of vaccination, has been decreased since the revision of the Law. Our current study suggests that the percentage of children with negative NTAb titers would increase to about 18% at 5 years after the second series of vaccination (at the age of 14 to 15) if the third series of vaccination was not pro-

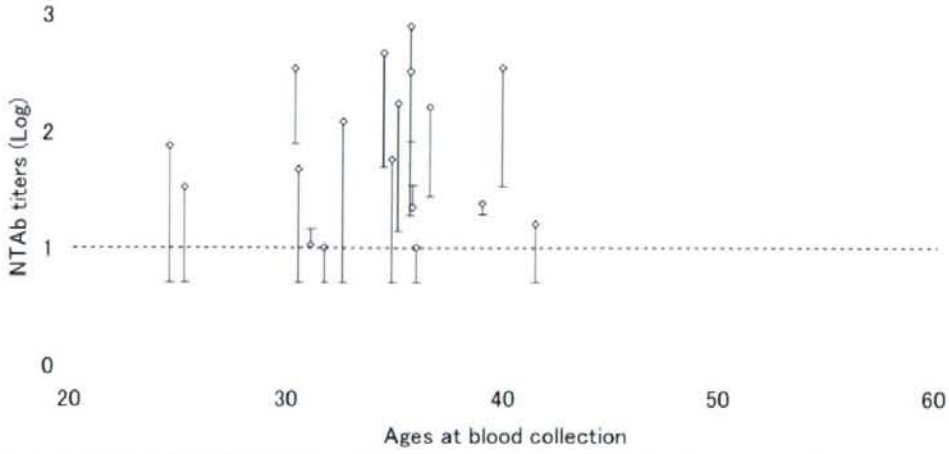

Fig. 6. Distribution of NTAb titers before additional vaccination: — and that of NTAb titers after additional vaccination: ◇ in adults serum samples (n=18). Neutralizing antibody titer in a NTAb negative sample is shown as 0.7.

vided. One of the paired serum samples (n=17) was found to be NTAb negative at only 3 years after the second series of routine vaccination. Therefore, it is at least highly possible that some children will not be able to maintain the sufficient NTAb titers of 1:10 to prevent JEV infection described by the WHO (27, 29), due to discontinuation of the third series of routine vaccination. Fortunately, no JE patient in the late teens was reported in the first year after MHLW decided to discontinue the third series of vaccination. Considering the pre-vaccination NTAb positive rate of 0.2% (data not shown) among children aged 6 to 90 months (n=468) shown in our previous phase III study of the Vero cell-derived JE vaccine, JE infection risk for children in the present-time Japan is presumably not very high. That children now have fewer chances to get bitten by mosquitoes may be another factor for the low risk of JE infection. However, the infection rate among swine is still high (6, 9). In 2006, 7 JE patients, including a 3-year-old, were identified. According to a study report, the JE virus was detected in the cerebrospinal fluid of 4 of 57 patients with aseptic meningitis (aged 2 to 6) (11). Although the vaccination history of the patients with aseptic meningitis was unknown, the data suggest that the risk of JEV infection is still a matter of concern. The predominant JEV genotype that shifted from Type III to Type I in Japan may have been causing the change of clinical symptoms associated with JE from encephalitis to meningitis (17). Assessment of JE infection risk is quite complicated as described earlier.

We expected to see many antibody-negative adults based on our previous data. In the phase I study of the Vero cell-derived JE vaccine conducted in 2001 in adult male volunteers living in Osaka City, Japan, aged between 20 and 35, 34.2% (92/269) of the volunteers were antibody negative (12), which is comparable to that shown in the analysis of adult serum samples in the current study. However, the actual antibody negative rate in the serum samples of 38 adult volunteers was slightly lower than the antibody negative rate estimated in the serum analysis of 17 children. Specifically, the antibody negative rate shown in the analysis of adult serum samples was 50.0% in volunteers under 30, 29.6% in those aged 30 or above and under 40, and 71.4% in those aged 40 or above. On the other hand, the estimated antibody negative rate shown in the analysis of serum samples collected from 17 children was 82% at 15 years post-vaccination (at the age of 24 to 25) and 100% at 20 years post-vaccination (at the age of 29 to 30). The slight difference in antibody negative rate was possibly caused by several factors. Approximately half of the adult volunteers had presumably received the third series of vaccination considering the third series vaccination rate of about 50% according to MHLW, although the vaccination history of the volunteers is unknown as described earlier. Some may have previously received JE vaccination prior to their past overseas travel. Some may have acquired natural immunity in Fukuoka, Japan, which is considered a high risk area for infection by JEV judging from the antibody prevalence in swine (6, 9). A linear decrease of NTAbs was assumed in the logarithmic scale since only single or paired serum samples collected from the children were used in the current study; however, decrease in acquired antibodies may be shown by a gentle curve (20). Thus, a complex association of these

factors may have caused the lower antibody negative rate among adults compared to the estimate based on the analysis of pediatric serum samples.

Epidemiological problems associated with the fact that 39.5% of the adult volunteers did not maintain the sufficient NTAb titers to prevent infection described by WHO (27, 29) cannot be ignored at any rate. We measured NTAb titers in serum samples of 18 adult volunteers after the additional vaccination and confirmed that all 8 volunteers who had been NTAb negative eventually turned positive. Based on the estimate that about 18% of children who received the second series of routine vaccination turn NTAb negative at 5 years post-vaccination (at the age of 14 to 15) and the analysis of paired serum samples that identified a child who turned NTAb negative at 3 years post-vaccination, additional vaccinations at intervals of at least 5 years after the second series of vaccination would be ideal in terms of maintaining the sufficient NTAb titers to prevent JEV infection. However, NTAb titers in adults after the additional vaccination became around $1:10^2$ as shown in Fig. 6, suggesting a smaller booster effect compared to that on children. Our previous phase I and III studies also showed comparable results. In the phase I study in adult male volunteers aged between 20 and 35, GMT after three series of vaccination was $1:10^{2.35}$ (n=30) with the Vero cell-derived vaccine and $1:10^{2.03}$ (n=28) with the current mouse brain-derived vaccine (12). On the other hand, GMT after three series of vaccination was $1:10^{3.96}$ (n=218) with the Vero cell-derived vaccine and $1:10^{3.76}$ (n=221) with the current vaccine in the phase III study in children aged between 6 to 90 months (data not shown). Children appear to be able to maintain higher NTAb titers that may decrease with age. It may be explained by the inferior booster effect from aging as shown in the case of the influenza vaccination (5). Affected by global warming, the risk of JEV infection in Japan will have little chance of decreasing in the future. The JE vaccine is also considered as a travelers' vaccine, and additional vaccinations are at least strongly recommended for adults who are scheduled to travel to Southeast Asia. Moreover, there is no information regarding the duration of the NTAb titer after additional vaccination in adults. It is suspected that the duration is shorter in adults than in children, because acquired NTAb titers in adults were, after additional vaccination, lower than in children as mentioned above. Therefore, investigation of the duration of NTAb titers in the adult population after additional vaccination would be meaningful in view of the risks related to infections in the elderly and travel to endemic areas.

The duration of NTAb titer in paired serum samples alone (n=17) estimated by using a random coefficient model was different from the duration in paired serum samples and additional single serum samples combined (n=47). Estimated value based on a random coefficient model is generally interpreted as weighted mean of population mean profile and data profile. The difference in estimated duration of NTAb titer in the two sets of serum samples is therefore considered as the result of underestimation of the random effect of additional single serum samples and increased weight of observation profile due to sample size increase. However, the estimated duration of NTAb titer in paired serum samples alone (n=17) is assumed to be more reliable than the estimated duration in paired serum samples and additional single serum samples combined (n=47) since the random coefficient model ignored within-subject variability in the data from the additional single serum samples (n=30).

Various methods have been proposed for statistical estimation of duration of antibody titers (24–26). A common problem associated with all the proposed methods is that within-subject variability is ignored. We used the random coefficient model that incorporated a within-subject covariance structure in the current study to solve the problem by taking into account both fixed and random effects. A similar attempt has been made in the Bayesian random-effects model of Coursaget et al. (4) and the Piecewise linear model of Pigeon et al. (20).

The current study has certain limitations in itself since it was designed as a retrospective study in which a limited number of serum samples were used. Duration of NTAb titer will need to be evaluated in a well-designed prospective study in the future when a Vero cell-derived vaccine is introduced. The first series of routine vaccination program, in which 3 sessions of vaccinations are given, cannot be changed in order to ensure basic immunity against JEV. However, the second and third series of routine vaccination need to be reevaluated based on a domestic epidemiological surveillance of JE and a proper assessment of the necessity of the JE vaccine as a travelers' vaccine.

We are grateful to Ms. Naomi Sakata, Ms. Mari Fukuhara, Ms. Kanae Hisama and Ms. Hiroko Izawa for their excellent technical assistance. The authors are indebted to Mr. Michael Leoncavallo and Dr. Shinichi Abe for their helpful discussions.

References

1) Abe, M., Kuzuhara, S., and Kino, Y. 2003. Establishment of an analyzing method for a Japanese encephalitis virus neutralization test in Vero cells. Vaccine **21**: 1989–1994.
2) Abe, M., Shiosaki, K., Hammar, L., Sonoda, K., Xing, L., Kuzuhara, S., Kino, Y., and Cheng, R.H. 2006. Immuno-

logical equivalence between mouse brain-derived and Vero cell-derived Japanese encephalitis vaccines. Virus Res. **121**: 152–160.

3) Centers for Disease Control and Prevention. 1993. Inactivated Japanese encephalitis virus vaccine. Recommendations of the Advisory Committee on Immunization Practices (ACIP). MMWR **42** (No. RR-1): 1–15.
4) Coursaget, P., Yvonnet, B., Gilks, W., Wang, C., Day, N., Chiron, J., and Diop-Mar, I. 1991. Scheduling of revaccination against hepatitis B virus. Lancet **337**: 1180–1183.
5) Goodwin, K., Viboud, C., and Simonsen, L. 2006. Antibody response to influenza vaccination in the elderly: a quantitative review. Vaccine **24**: 1159–1169.
6) Halstead, S.B., and Tsai, T.F. 2004. Japanese encephalitis vaccines, p. 919–958. *In* Plotkin, S.A., and Orenstein, W.A. (eds), Vaccines, 4th ed, WB Saunders, Philadelphia, PA.
7) Hombach, J., Barrett, A.D., Cardosa, M.J., Deubel, V., Guzman, M., Kurane, I., Roehrig, J.T., Sabchareon, A., and Kieny, M.P. 2005. Review on flavivirus vaccine development. Proceedings of a meeting jointly organized by the World Health Organization and the Thai Ministry of Public Health, 26–27 April 2004, Bangkok, Thailand. Vaccine **23**: 2689–2695.
8) Hombach, J., Solomon, T., Kurane, I., Jacobson, J., and Wood, D. 2005. Report on a WHO consultation on immunological endpoints for evaluation of new Japanese encephalitis vaccines, WHO, Geneva, 2–3 September, 2004. Vaccine **23**: 5205–5211.
9) Kitano, T., and Oya, A. 1996. Japanese encephalitis vaccine, p. 103–113. *In* Arai, Y., Asano, T., Chino, F., Katow, S., Miyamura, T., Nakamura, R., Oya, A., and Sato, H. (eds), Vaccine handbook, Maruzen, Tokyo.
10) Kurane, I., and Takasaki, T. 2000. Immunogenicity and protective efficacy of the current inactivated Japanese encephalitis vaccine against different Japanese encephalitis virus strains. Vaccine **18 Suppl 2**: 33–35.
11) Kuwayama, M., Ito, M., Takao, S., Shimazu, Y., Fukuda, S., Miyazaki, K., Kurane, I., and Takasaki, T. 2005. Japanese encephalitis virus in meningitis patients, Japan. Emerg. Infect. Dis. **11**: 471–473.
12) Kuzuhara, S., Nakamura, H., Hayashida, K., Obata, J., Abe, M., Sonoda, K., Nishiyama, K., Sugawara, K., Takeda, K., Honda, T., Matsui, H., Shigaki, T., Kino, Y., Mizokami, H., Tanaka, M., Mizuno, K., and Ueda, K. 2003. Non-clinical and phase I clinical trials of a Vero cell-derived inactivated Japanese encephalitis vaccine. Vaccine **21**: 4519–4526.
13) Mackenzie, J. 2005. Emerging zoonotic encephalitis viruses: lessons from Southeast Asia and Oceania. J. Neurovirol. **11**: 434–440.
14) Mackenzie, J.S., Gubler, D.J., and Petersen, L.R. 2004. Emerging flaviviruses: the spread and resurgence of Japanese encephalitis, West Nile and dengue viruses. Nat. Med. **10**: S98–109.
15) Mackenzie, J.S., Johansen, C.A., Ritchie, S.A., van den Hurk, A.F., and Hall, R.A. 2002. Japanese encephalitis as an emerging virus: the emergence and spread of Japanese encephalitis virus in Australasia. Curr. Top. Microbiol. Immunol. **267**: 49–73.
16) Markoff, L. 2000. Points to consider in the development of a surrogate for efficacy of novel Japanese encephalitis virus vaccines. Vaccine **18 Suppl 2**: 26–32.
17) Nga, P.T., Del Carmen Parquet, M., Cuong, V.D., Ma, S.P., Hasebe, F., Inoue, S., Makino, Y., Takagi, M., Nam, V.S., and Morita, K. 2004. Shift in Japanese encephalitis virus (JEV) genotype circulating in northern Vietnam: implications for frequent introductions of JEV from Southeast Asia to East Asia. J. Gen. Virol. **85**: 1625–1631.
18) Ohtaki, E., Matsuishi, T., Hirano, Y., and Maekawa, K. 1995. Acute disseminated encephalomyelitis after treatment with Japanese B encephalitis vaccine (Nakayama-Yoken and Beijing strains). J. Neurol. Neurosurg. Psychiatr. **59**: 316–317.
19) Oya, A. 1988. Japanese encephalitis vaccine. Acta Paediatr. Jpn. **30**: 175–184.
20) Pigeon, J.G., Bohidar, N.R., Zhang, Z., and Wiens, B.L. 1999. Statistical models for predicting the duration of vaccine-induced protection. Drug Inform. J. **33**: 811–819.
21) Plesner, A.M. 2003. Allergic reactions to Japanese encephalitis vaccine. Immunol. Allergy Clin. North Am. **23**: 665–697.
22) Sugawara, K., Nishiyama, K., Ishikawa, Y., Abe, M., Sonoda, K., Komatsu, K., Horikawa, Y., Takeda, K., Honda, T., Kuzuhara, S., Kino, Y., Mizokami, H., Mizuno, K., Oka, T., and Honda, K. 2002. Development of Vero cell-derived inactivated Japanese encephalitis vaccine. Biologicals **30**: 303–314.
23) Tsai, T.F. 2000. New initiatives for the control of Japanese encephalitis by vaccination: minutes of a WHO/CVI meeting, Bangkok, Thailand, 13–15 October 1998. Vaccine **18 Suppl 2**: 1–25.
24) Van Damme, P., Thoelen, S., Cramm, M., De Groote, K., Safary, A., and Meheus, A. 1994. Inactivated hepatitis A vaccine: reactogenicity, immunogenicity, and long-term antibody persistence. J. Med. Virol. **44**: 446–451.
25) Wiedermann, G., Kundi, M., Ambrosch, F., Safary, A., D'Hondt, E., and Delem, A. 1997. Inactivated hepatitis A vaccine: long-term antibody persistence. Vaccine **15**(6/7): 612–615.
26) Wiens, B.L., Bohidar, N.R., Pigeon, J.G., Egan, J., Humi, W., Brown, L., Kuter, B.J., and Nalin, D.R. 1996. Duration of protection from clinical hepatitis A disease after vaccination with VAQTA. J. Med. Virol. **49**: 235–241.
27) World Health Organization. 2006. Weekly epidemiological record. Wkly. Epidemiol. Rec. **81**: 325–340.
28) World Health Organization. 2005. Weekly epidemiological record. Wkly. Epidemiol. Rec. **80**: 241–248.
29) World Health Organization. 1998. Weekly epidemiological record. Wkly. Epidemiol. Rec. **73**: 337–344.

JOURNAL OF VIROLOGY, Sept. 2007, p. 9653–9664
0022-538X/07/$08.00+0 doi:10.1128/JVI.00568-07

Vol. 81, No. 18

Enhanced Phosphorylation of Transcription Factor Sp1 in Response to Herpes Simplex Virus Type 1 Infection Is Dependent on the Ataxia Telangiectasia-Mutated Protein▽

Satoko Iwahori,[1] Noriko Shirata,[1] Yasushi Kawaguchi,[2] Sandra K. Weller,[3] Yoshitaka Sato,[1] Ayumi Kudoh,[1] Sanae Nakayama,[1] Hiroki Isomura,[1] and Tatsuya Tsurumi[1]*

Division of Virology, Aichi Cancer Center Research Institute, 1-1, Kanokoden, Chikusa-ku, Nagoya 464-8681, Japan[1]; Institute of Medical Science, University of Tokyo, Shirokanedai, Minato-ku, Tokyo 108-8639, Japan[2]; and Department of Molecular, Microbial and Structural Biology MC3205, University of Connecticut Health Center, 263 Farmington Avenue, Farmington, Connecticut 06030[3]

Received 19 March 2007/Accepted 26 June 2007

The ataxia telangiectasia-mutated (ATM) protein, a member of the related phosphatidylinositol 3-like kinase family encoded by a gene responsible for the human genetic disorder ataxia telangiectasia, regulates cellular responses to DNA damage and viral infection. It has been previously reported that herpes simplex virus type 1 (HSV-1) infection induces activation of protein kinase activity of ATM and hyperphosphorylation of transcription factor, Sp1. We show that ATM is intimately involved in Sp1 hyperphosphorylation during HSV-1 infection rather than individual HSV-1-encoded protein kinases. In ATM-deficient cells or cells silenced for ATM expression by short hairpin RNA targeting, hyperphosphorylation of Sp1 was prevented even as HSV-1 infection progressed. Mutational analysis of putative ATM phosphorylation sites on Sp1 and immunoblot analysis with phosphopeptide-specific Sp1 antibodies clarified that at least Ser-56 and Ser-101 residues on Sp1 became phosphorylated upon HSV-1 infection. Serine-to-alanine mutations at both sites on Sp1 considerably abolished hyperphosphorylation of Sp1 upon infection. Although ATM phosphorylated Ser-101 but not Ser-56 on Sp1 in vitro, phosphorylation of Sp1 at both sites was not detected at all upon infection in ATM-deficient cells, suggesting that cellular kinase(s) activated by ATM could be involved in phosphorylation at Ser-56. Upon viral infection, Sp1-dependent transcription in ATM expression-silenced cells was almost the same as that in ATM-intact cells, suggesting that ATM-dependent phosphorylation of Sp1 might hardly affect its transcriptional activity during the HSV-1 infection. ATM-dependent Sp1 phosphorylation appears to be a global response to various DNA damage stress including viral DNA replication.

Transcription factor Sp1 is a 95- to 105-kDa protein that binds to GC-rich recognition elements (GC-boxes) through C-terminal zinc finger motifs (30). Sp1 functions as a transactivator of gene expression, and its recognition elements are distributed widely in various promoters of cellular and viral genes (15, 16, 19). As with many other transcription factors, the transcription activity of Sp1 is regulated in part by post-translational modifications, which include phosphorylation, glycosylation, acetylation, and sumoylation (5, 9, 26, 54). It has been recently demonstrated that phosphorylation of Sp1 alters its transcription activity in a wide variety of physiological processes, including cell cycle progression, terminal differentiation, and viral infection (2, 9, 17, 23, 28, 36, 41). Also, relationships between the phosphorylation site(s) on Sp1 and specific kinases have been clarified, with documentation of targeting of Ser-59 by cyclin A-CDK, Ser-220 (quoted as Ser-131 in the original study) by DNA-dependent protein kinase (DNA-PK), Thr-453 and Thr-739 by p42/p44 mitogen-activated protein kinase (MAPK), and Thr-668 (quoted as Thr-579 in the original study) by casein kinase II (2, 9, 11, 17, 41). Cyclin A-CDK-mediated phosphorylation increases DNA-binding activity of Sp1 (17, 23). Inactivation of Thr-453 and Thr-739 phosphorylation sites by p42/p44 MAPK decreases by half the transcriptional activity (41). Mutation of the Thr-668 phosphorylation site which is in the Zinc finger motif of Sp1 increases its DNA-binding activity, further suggesting that casein kinase II-mediated phosphorylation decreases DNA-binding activity of Sp1 (2).

Phosphorylation of Sp1 upon virus infection has been reported in several studies (9, 11, 28, 31). For example, simian virus 40 infection induces both increased levels and phosphorylation of Sp1 (28). In a study of human immunodeficiency virus type 1 (HIV-1) infection, it was shown that the HIV-1-encoded Tat protein promotes DNA-PK-dependent Sp1 phosphorylation in vitro, which is associated with increased transcription activity (11).

Herpes simplex virus type 1 (HSV-1) is a large, enveloped virus with 152-kbp double-stranded DNA encoding approximately 84 proteins (39, 49). During productive replication, cascade regulation of gene expression occurs, based on stepwise activation of immediate-early, early, early late, and late promoters (24). The promoters of different expression kinetics classes are equipped for binding of not only viral transcription factors but also various cellular transcription factors, including Sp1. Sp1-binding sites are frequently found in promoters of immediate-early and early genes (48, 57), suggesting a pivotal

* Corresponding author. Mailing address: Division of Virology, Aichi Cancer Center Research Institute, 1-1, Kanokoden, Chikusa-ku, Nagoya 464-8681, Japan. Phone and fax: 81-52-764-2979. E-mail: ttsurumi@aichi-cc.jp.

▽ Published ahead of print on 3 July 2007.

function of Sp1 in gene expression of HSV-1. HSV-1 infection induces hyperphosphorylation of Sp1 at early stages of infection without any significant change in abundance (31). While the DNA-binding activity of Sp1 was found to be unchanged until 8 h postinfection (hpi), purified Sp1 from HSV-1-infected cells at 12 hpi had reduced transcription activity in vitro (31). However, the kinase(s) responsible for Sp1 phosphorylation induced by HSV-1 infection have remained unclear.

We and others previously reported that HSV-1 infection induces a cellular DNA damage response, with activation of the ATM signal transduction pathway (37, 53, 60). The activated form of ATM phosphorylated at Ser-1981 and the DNA damage sensor Mre11-Rad50-Nbs1 complex are recruited and retained in viral replication compartments, where transcription and replication of viral genes take place. Activation of the ATM-Rad3-related (ATR) replication checkpoint pathway, in contrast, is minimal. ATM is a member of the related phosphatidylinositol 3 (PI-3)-like kinase family, as well as ATR and DNA-PK, and displays kinase activity against serine and threonine, followed by glutamine, generally responding to a genotoxic stress such as ionizing radiation (IR) (1, 6, 12, 13, 52).

In the present report, we provide evidence for considerable ATM involvement in the hyperphosphorylation of Sp1 during HSV-1 infection rather than individual HSV-1-encoded PKs. In ATM-deficient cells or cells silenced for ATM expression by short hairpin RNA (shRNA) targeting, the levels of the hyperphosphorylated form of Sp1 did not increase even as HSV-1 infection progressed. Using mutational analysis and immunoblotting with phosphopeptide-specific antibodies, we have identified that at least Ser-56 and Ser-101 on Sp1 became phosphorylated in response to HSV-1 infection. Although ATM phosphorylated Ser-101 but not Ser-56 on Sp1 in vitro, phosphorylation of Sp1 at both sites was not detected at all upon infection in ATM-deficient cells, suggesting that other cellular kinase(s) activated by ATM could be involved in phosphorylation at Ser-56. Upon viral infection Sp1-dependent transcription in ATM expression-silenced cells was almost the same as that in ATM-intact cells, suggesting that ATM-dependent phosphorylation of Sp1 might hardly affect its transcriptional activity during viral infection. Since it is known that HSV-1 infection decreases transcriptional activity of Sp1 (31), modification(s) of Sp1 besides ATM-dependent phosphorylation might affect its transcriptional activity.

MATERIALS AND METHODS

Cells. HeLa, HFF2 (human foreskin fibroblasts immortalized by introduction of the human telomerase reverse-transcriptase [*hTERT*] gene [56]), and 293T cells were grown and maintained at 37°C in Dulbecco modified Eagle medium (DMEM; Sigma) supplemented with 10% fetal calf serum (FCS). Human glioma cell lines M059J and MJ-M6 (34) were maintained in DMEM–Ham F-12 nutrient mixture (Sigma) supplemented with 10% FCS and puromycin (0.5 μg/ml). Skin fibroblasts from ataxia telangiectasia patients immortalized by introduction of *hTERT* gene (AT10S/T-n cells) were maintained at 37°C in DMEM supplemented with 10% FCS and G418 (200 μg/ml) (43). The 293T cells were infected with retroviruses expressing ATM shRNA or control retroviruses and selected (56). The resultant 293T cells stably expressing ATM shRNA (293T-ATM shRNA) or the control vector cells (293T-Control vector) were maintained at 37°C in DMEM supplemented with 10% FCS and hygromycin B (100 μg/ml) (56). Sf9 and SF21 cells were maintained at 27°C in Sf-900 II (Gibco) supplemented with 10% FCS.

Viruses. HSV-1 strain 17+ was used throughout the experiments. A Us3-deficient virus, R7041 (46), and a UL13-deficient virus, R7356 (47), derived from HSV-1 strain F were kindly provided by B. Roizman. The UL39-deficient virus, ICP6Δ, derived from HSV-1 strain KOS was from a collaborator, S. K. Weller (20). Infection was performed on monolayers of cultured cells at the indicated multiplicities of infection (MOIs). After 1 h adsorption at 37°C, inoculum was removed, and monolayers were overlaid with fresh medium.

TABLE 1. Primer sets for construction of serine/threonine-to-alanine mutations by site-directed mutagenesis

Mutation site	Sequences of paired primers (5′–3′)
S36A	GGTGGTGCCTTTGCACAGGCTCGAA
	TTCGAGCCTGTGCAAAGGCACCACC
S56A	GGAGGGCAGGAGGCCCAGCCATCCC
	GGGATGGCTGGGCCTCCTGCCCTCC
S81A	AGAACAGCAACAACGCCCAGGGCCCGAGTC
	GACTCGGGCCCTGGGCGTTGTTGCTGTTCT
S85A	CTCCCAGGGCCCGGCTCAGTCAGGGGGAAC
	GTTCCCCCTGACTGAGCCGGGCCCTGGGAG
T98A	GACCTCACAGCCGCACAACTTTCAC
	GTGAAAGTTGTGCGGCTGTGAGGTC
S101A	GCCACACAACTTGCACAGGGTGCCA
	TGGCACCCTGTGCAAGTTGTGTGGC
T250A	CTCTCAGGACAGGCTCAGTATGTGA
	TCACATACTGAGCCTGTCCTGAGAG
S281A	CCTTGACTCCCAGCGCTCAGGCAGTCACGA
	TCGTGACTGCCTGAGCGCTGGGAGTCAAGG
S291A/S296A	AGCAGCTCTGGGGCCCAGGAGAGTGGCGC
	ACAGCCTGTCA
	TGACAGGCTGTGCGCCACTCTCCTGGGCCCC
	AGAGCTGCT
S313A	AGCTTGGTATCAGCACAAGCCAGTT
	AACTGGCTTGTGCTGATACCAAGCT
S351A	TCAGGGACCAACGCTCAAGGCCAGA
	TCTGGCCTTGAGCGTTGGTCCCTGA
T394A	CAAAACCAGCAGGCACAGCA
	TGCTGTGCCTGCTGGTTTTG
T427A/S431A	GGGCAGACCTTTGCAGCTCAAGCCATCGCC
	CAGGAAACCC
	GGGTTTCCTGGGCGATGGCTTGAGCTGCAA
	AGGTCTGCCC

Plasmids. For subcloning of Sp1 gene into pFastBac1 (Invitrogen) containing a sequence (RGS-6xHis-Flag) supplied by W. Nakai, two primers (5′-GGAATTCCATATGGGATGAAATGACAGCTGTGG-3′ and 5′-GCTCTAGATCAGAAGCCATTGC-3′) were designed. Plasmid CMV-hSp1 (22) supplied from G. Suske was used as a template for PCR. The PCR product was double digested by NdeI and XbaI and subcloned into pFastBac1 containing a sequence (RGS-6xHis-Flag), and the resultant plasmid was designated pFB-RHF/Sp1. For construction of a mammalian expression vector for Sp1, two primers (5′-TTATAATAGGGGTACCCCACCATGCGCGG-3′ and 5′-GCTCTAGAGCTCAGAAGCCA-3′) were designed. pFB-RHF/Sp1 was used as a template for PCR. The PCR product was double digested by KpnI and XbaI and subcloned into pcDNA3.1(+) (Invitrogen), and the resultant plasmid was designated pcDNA-RHF/Sp1. Serine/threonine-to-alanine mutations were constructed with a QuikChange site-directed mutagenesis kit (Stratagene) using the primer sets given in Table 1. Multiple mutations were introduced by repetition. The plasmids were designated pcDNA-RHF/Sp1-S36A, pcDNA-RHF/Sp1-S56A, pcDNA-RHF/Sp1-S81A, pcDNA-RHF/Sp1-S85A, pcDNA-RHF/Sp1-T98A, pcDNA-RHF/Sp1-S101A, pcDNA-RHF/Sp1-T250A/S281A, pcDNA-RHF/Sp1-S291/296A, pcDNA-RHF/Sp1-S313A, pcDNA-RHF/Sp1-S351A, pcDNA-RHF/Sp1-T394A, pcDNA-RHF/Sp1-T427A/S431A, pcDNA-RHF/Sp1-S56/81/85A, pcDNA-RHF/Sp1-S56/101A, pcDNA-RHF/Sp1-S56A/T250A, and pcDNA-RHF/Sp1-S56/281A, and all mutations were confirmed by sequencing.

For subcloning of a glutathione *S*-transferase (GST) fusion protein with truncated Sp1 (8 to 167 amino acids), two primers (5′-CGGGATCCCGTATGGATGAAATGAC-3′ and 5′-ACTCTCGAGCACTCCAGGTAGT-3′) were designed, and pcDNA-RHF/Sp1, pcDNA-RHF/Sp1-S56A, pcDNA-RHF/Sp1-S101A, and pcDNA-RHF/Sp1-S56/101A were used as templates for PCR. The PCR products were double digested with BamHI and XhoI and subcloned into pGEX-6P-3 (Amersham Biosciences). The plasmids were designated pGEX-6P-$Sp1_{8\text{-}167}$, pGEX-6P-$Sp1_{8\text{-}167}$-S56A, pGEX-6P-$Sp1_{8\text{-}167}$-S101A, and pGEX-6P-$Sp1_{8\text{-}167}$-S56/101A.

Purification of recombinant Sp1 from insect cells. Purification of recombinant His_6 flag-tagged Sp1 from insect cells was carried out with a Bac-to-Bac system (Invitrogen). DH10Bac *Escherichia coli* cells were transformed with pFB-RHF/

Sp1, and the resultant bacmid was transfected into Sf9 cells using Lipofectin reagent (Invitrogen). The obtained virus was designated AcRHF/Sp1. SF21 cells (5×10^7) were infected with AcRHF/Sp1 at an MOI of 5. At 60 hpi, the cells were harvested, suspended in a buffer (50 mM Tris-HCl [pH 8], 1% Nonidet P-40 [NP-40], 250 mM NaCl, 10 mM 2-mercaptoethanol [2-ME], 1 mM phenylmethylsulfonyl fluoride [PMSF]), sonicated, and centrifuged. The clarified lysate was combined with Ni-NTA (QIAGEN). After rotation for 2 h, the beads were washed twice with buffer A (20 mM Tris-HCl [pH 8], 10% glycerol, 10 mM 2-ME) containing 500 mM KCl and 20 mM imidazole, once with buffer A containing 1 M KCl, once with buffer A containing 500 mM KCl and 20 mM imidazole, and twice with buffer A containing 100 mM KCl and 20 mM imidazole and then eluted with buffer A containing 100 mM KCl and 100 mM imidazole. The eluted protein was dialyzed against dialysis buffer (20 mM Tris-HCl [pH 8], 100 mM NaCl, 20% glycerol, and 1 mM PMSF) and combined with anti-Flag M2 affinity gel (Sigma). After rotation for 3 h, the beads were washed three times with TBS + buffer (50 mM Tris-HCl [pH 8], 150 mM NaCl, 1 mM EDTA, 0.1% NP-40, 10% glycerol, 1 mM PMSF), and the protein was eluted with 0.1 M glycine (pH 3.5), neutralized immediately, dialyzed against dialysis buffer, and stored at −80°C.

Purification of recombinant Sp1 from bacteria. *E. coli* (BL21) transformed with pGEX-6P-$Sp1_{8-167}$, pGEX-6P-$Sp1_{8-167}$-S56A, pGEX-6P-$Sp1_{8-167}$-S101A, and pGEX-6P-$Sp1_{8-167}$-S56/101A were cultured at 30°C until the optical density at 600 nm reached 0.6, and IPTG (isopropyl-β-D-thiogalactopyranoside) was added at a final concentration of 1 mM. After 5 h of incubation, the collected cells were suspended in GLB buffer (50 mM Tris-HCl [pH 7.4], 50 mM glucose, 1 mM EDTA, 10 mM 2-ME, 1 mM PMSF, 0.2% NP-40). After sonication, the lysate was clarified by centrifugation, combined with glutathione-Sepharose 4B (Amersham Biosciences), and rotated at 4°C for 90 min. After three washes with GLB containing 0.2% NP-40, the proteins were eluted with elution buffer (10 mM reduced glutathione, 50 mM Tris-HCl [pH 8], 1 mM PMSF) and dialyzed against dialysis buffer. The purified proteins were designated GST-$Sp1_{8-167}$, GST-$Sp1_{8-167}$-S56A, GST-$Sp1_{8-167}$-S101A, and GST-$Sp1_{8-167}$-S56/101A.

IP-kinase assays. Immunoprecipitation (IP)-kinase assays were performed with some modification as described previously (6, 10, 32). 293T cells (5×10^6) were transfected with either pcDNA-Flag-ATMwt or pcDNA-Flag-ATMkd (5 μg of each; kind gifts from M. B. Kastan [6]) using Lipofectamine 2000 (Invitrogen). At 48 h posttransfection, cells were harvested, rinsed with ice-cold phosphate-buffered saline, lysed with lysis buffer (20 mM Tris-HCl [pH 7.4], 150 mM NaCl, 1 mM EDTA, 0.5% Triton X-100 [TX-100], 5% glycerol, 1 mM PMSF, 100 mM NaF, 2 mM Na_3VO_4, and complete protease inhibitor [Roche]), incubated for 15 min on ice, sonicated, and clarified by centrifugation. Cell lysates (2 mg) were incubated with anti-Flag M2 affinity resin (20 μl of suspension) and rotated for 3 h at 4°C. The immunocomplex was washed three times with lysis buffer containing 0.65% TX-100, twice with Tris-LiCl buffer (100 mM Tris-HCl [pH 7.5], 0.5 M LiCl, 1 mM NaF, 1 mM Na_3VO_4) and once with kinase buffer (10 mM HEPES [pH 7.9], 50 mM glycerophosphate, 50 mM NaCl, 10 mM $MgCl_2$, 10 mM $MnCl_2$, 1 mM dithiothreitol, 1 mM NaF, and 1 mM Na_3VO_4) containing 5 μM ATP. For activation of ATM, the immunocomplex was incubated with kinase buffer containing 1 mM ATP for 30 min at 30°C. After incubation, the immunocomplex was washed three times with kinase buffer containing 5 μM ATP and divided into two portions for kinase reactions with either purified Sp1 or p53 as substrate. Kinase reactions were carried out by resuspending the immunocomplex in kinase buffer containing 10 μCi [γ-^{32}P]ATP and either 500 ng of Sp1 purified from insect cells or 250 ng of p53 (Active Motif), followed by incubation for 30 min at 30°C. The reactions were terminated by addition of sodium dodecyl sulfate (SDS) gel loading buffer, and the samples were separated by SDS–10% polyacrylamide gel electrophoresis (PAGE), followed by autoradiography. In the case of GST-$Sp1_{8-167}$, GST-$Sp1_{8-167}$-S56A, GST-$Sp1_{8-167}$-S101A, and GST-$Sp1_{8-167}$-S56/101A, 1 μg of each protein was used as a substrate.

Antibodies. Primary antibodies were purchased from Santa Cruz (Sp1 PEP2), Abcam (HSV-1 ICP4, UL42), GeneTex (ATM-2C1), Cell Signaling Technology (ATM-S1981), Ambion (GAPDH [glyceraldehyde-3-phosphate dehydrogenase]), Sigma (Flag M2), and Biosource (DNA-dependent PK catalytic subunit). Phosphopeptide-specific rabbit antibodies were raised against serine-56 phosphopeptide, CGGGQEpSQPSP1, for anti-Sp1 (pS56) and serine-101 phosphopeptide, CTATQLpSQGANG, for anti-Sp1 (pS101), conjugated with KLH. Antibodies were purified through the specific phosphopeptide-conjugated columns and passed through the corresponding unphosphorylated peptide-conjugated columns.

Transient-transfection and infection. HeLa cells (6×10^5) were transfected with 0.8 μg of pcDNA-RHF/Sp1 or expression vectors of mutated Sp1 using Lipofectamine 2000. At 24 h posttransfection, the transfected cells were infected with HSV-1 at an MOI of 10. At 24 hpi, the cells were harvested and subjected to immunoblot analysis.

IP. HeLa cells transfected with pcDNA-RHF/Sp1, pcDNA-RHF/Sp1-S56A, or pcDNA-RHF/Sp1-S101A were infected with HSV-1 at an MOI of 10. At 24 hpi, the cells were harvested, suspended in lysis buffer (50 mM Tris-HCl [pH 7.4], 150 mM NaCl, 1 mM EDTA, 1% TX-100, 100 mM NaF, 2 mM Na_3VO_4, and protease inhibitor cocktail [Sigma]), and centrifuged. The clarified lysate was combined with anti-Flag M2 affinity resin and rotated for 3 h at 4°C. The immune complex was washed three times with TBS buffer (50 mM Tris-HCl [pH 7.4], 150 mM NaCl), and eluted with SDS gel loading buffer.

Immunoblot analysis. HeLa, HFF2, M059J, MJ-M6, and AT10S/T-n cells were suspended in lysis buffer (20 mM Tris-HCl [pH 7.4], 0.5% TX-100, 300 mM NaCl, 1 mM EDTA, 0.1% SDS, 100 mM NaF, 2 mM Na_3VO_4, protease inhibitor cocktail [Sigma]) and incubated on ice for 40 min, followed by centrifugation to obtain clarified supernatants. 293T-ATM shRNA and 293T-Control vector cells were suspended in urea buffer (8 M urea, 0.1 M NaH_2PO_4, 10 mM Tris [pH 8]), sonicated, and centrifuged. For experiments with alkaline phosphatase treatment, HFF2 and HeLa cells were infected with HSV-1 and harvested at 10 and 12 hpi, respectively. Cells were suspended in AP buffer (50 mM Tris-HCl [pH 8], 0.5 M NaCl, 2% NP-40, protease inhibitor cocktail [Sigma]), stored on ice for 30 min, and then centrifuged. Whole-cell lysates (20 μg) were incubated in a reaction mixture containing 10 U of calf intestinal alkaline phosphatase (CIAP; New England Biolabs) and 10 mM $MgCl_2$ for 30 min at 37°C. Equal amounts of proteins (2.5 to 30 μg) were separated by 7.5% (acrylamide [A]:bisacrylamide [B] = 72:1) or 10% (A:B = 30:0.8) SDS-PAGE and transferred onto Immobilon transfer membranes (Millipore). Immunoreactivity was detected by Western Lightning (Perkin-Elmer). Images were processed by LumiVision PRO 400EX (Aisin/Taitec, Inc.). Signal intensity was quantified with LumiVision Analyzer 400. The system used in the present study mounts the cooled charge-coupled device camera that has 16 bit = 65,535 grayscale wide dynamic range. It enhances the accuracy of the quantitative analysis up to 100 times compared to the ordinary quantitative analysis scanning an X-ray film into the personal computer after exposing the signal to the film.

IR. HFF2 cells were exposed to gamma irradiation with 10 Gy and harvested at 15 min after radiation. 293T-ATM shRNA and 293T-Control vector cells were exposed to gamma irradiation with 20 Gy and harvested at 15 min after radiation.

CAT assays. Chloramphenicol acetyltransferase (CAT) assays were carried out as described previously (27, 62). All transfections were in triplicate on 35-mm-diameter plates of 293T-ATM shRNA or 293T-Control vector cells (1.2×10^6) with either p65F1CAT (3.5 μg; a gift from A. D. Yurochko) (62) or pCAT TATA+Sp1(−55)+Sp1 (−75) (1 μg) (27) using Lipofectamine 2000 according to the manufacturer's instructions. At 24 h posttransfection, cells were infected with HSV-1 at an MOI of 5 and harvested at 12 hpi. Cell lysates were then prepared and subjected to CAT assays as described previously (27, 62). Equal amounts of proteins from each sample [0.4 μg for p65F1CAT-transfected cells, 0.2 μg for pCAT TATA+Sp1(−55)+Sp1(−75)-transfected cells] were assayed for CAT activity. Acetylated and unacetylated [^{14}C]chloramphenicol (Amersham Biosciences) were separated by thin-layer chromatography in a chloroform-methanol (95:5) solvent. Images were obtained using a BAS2500 Image Reader (Fujifilm), the signal intensities were quantified with an Image Gauge, and the levels of activity were analyzed by calculating the percentage of the conversion of unacetylated [^{14}C]chloramphenicol to the acetylated form.

RESULTS

Hyperphosphorylation of Sp1 is induced upon HSV-1 infection. In order to confirm whether transcription factor Sp1 is hyperphosphorylated upon HSV-1 infection as reported previously (31), HeLa and HFF2 cells were infected with HSV-1. As shown in Fig. 1A, most of the Sp1 proteins were converted to slower-migrating forms in SDS-PAGE by 4 hpi in HeLa cells. Similarly, the slower-migrating forms of Sp1 in HFF2 cells became the major form by 4 hpi (Fig. 1C). CIAP treatment of the lysates from HSV-1-infected HeLa cells (Fig. 1B) or HFF2 cells (Fig. 1D) changed the slower-migrating forms of Sp1 to the faster-migrating form. Thus, Sp1 became hyperphosphorylated after HSV-1 infection without a significant change in abundance, confirming the previous finding (31).

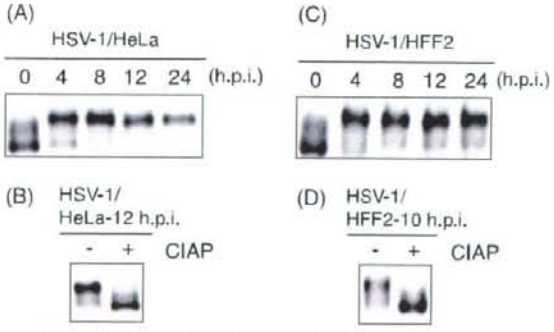

FIG. 1. Hyperphosphorylation of Sp1 is induced upon HSV-1 infection. HeLa (A) and HFF2 cells (C) were infected with HSV-1 at MOIs of 10 and 5, respectively, and were harvested at the indicated times postinfection. Whole-cell lysates were prepared, and equal amounts of proteins from each sample (2.5 or 30 μg) were subjected to immunoblot analysis with anti-Sp1 antibody. (B and D) Whole-cell lysates obtained from HSV-1-infected HeLa and HFF2 cells at the indicated times postinfection were treated with (+) or without (−) CIAP for 30 min at 37°C. The samples were subjected to immunoblot analysis with anti-Sp1 antibody.

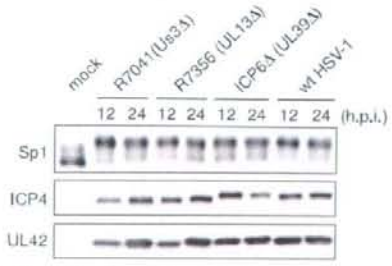

FIG. 2. Hyperphosphorylation of Sp1 is induced even upon infection of HSV-1 mutants defective for viral PK, Us3, UL13 or UL39 gene product. HFF2 cells were infected with wild-type HSV-1 (wt HSV-1), Us3-defective virus (R7041), UL13-defective virus (R7356), or UL39-defective virus (ICP6Δ) at an MOI of 5. At 12 and 24 hpi, cells were harvested and whole-cell lysates were prepared. Equal amounts of proteins from each sample (15 μg) were subjected to immunoblot analysis with anti-Sp1, ICP4, and UL42 proteins specific antibodies. Mock, mock infection.

Hyperphosphorylation of Sp1 is induced even upon infection of HSV-1 mutants defective for viral PK, Us3, UL13, or UL39 gene product. HSV-1 expresses at least three viral PKs encoded by the Us3, UL13, and UL39 genes (20, 46, 47). To examine whether Us3, UL13, or UL39 viral PK is involved in the Sp1 hyperphosphorylation, we investigated the phosphorylation state of Sp1 in HFF2 cells infected with wild type, Us3-deficient (R7041), UL13-deficient (R7356), or UL39 (viral ribonucleotide reductase large subunit)-deficient (ICP6Δ) virus (Fig. 2). The expression levels of the virus-encoded immediate-early protein (ICP4) and early protein (UL42) were almost the same among wild-type- and the mutant virus-infected cells. Since R7041 and R7356 are derived from HSV-1 strain F (46, 47) and ICP6Δ is from HSV-1 strain KOS (20), it is possible that the different gel mobilities of ICP4 proteins among wild-type HSV-1 (strain 17+) and the mutant viruses could be due to interstrain variabilities. Sp1 proteins in HFF2 cells infected with Us3-deficient (R7041), UL13-deficient (R7356), or UL39-deficient (ICP6Δ) viruses were mainly detected as hyperphosphorylated forms (the slower-migrating forms) by 12 hpi, as in the case of wild-type HSV-1 (Fig. 2). These results indicate that HSV-1 encoded PKs are not individually involved to any large extent in Sp1 hyperphosphorylation induced upon HSV-1 infection. However, the possibility of redundancy among some combination of these three PKs in Sp1 phosphorylation could not be excluded.

Activated ATM is involved in hyperphosphorylation of Sp1 upon HSV-1 infection. The HSV-1 infection activates ATM and elicits an ATM-dependent DNA damage signal transduction in infected cells (37, 53, 60). Since Sp1 possesses 15 putative phosphorylation sites targeted by ATM as estimated from the motifs (see Fig. 5A), we therefore examined phosphorylation states of Sp1 in ATM expression-silenced 293T cells infected with HSV-1 (Fig. 3A). The 293T cells stably expressing the ATM gene-targeted shRNA (293T-ATM shRNA) or the control vector cells (293T-Control vector) (53, 56) were infected with HSV-1. The expression level of ATM was very low in 293T-ATM shRNA cells compared to that in 293T-Control vector cells. In 293T-Control vector cells, most of the Sp1 proteins were hyperphosphorylated to slower-migrating forms by 5 hpi (Fig. 3A). In contrast, in 293T-ATM shRNA cells part of the Sp1 protein was converted to hyperphosphorylated forms, but 44% of Sp1 still remained as the faster-migrating form even at 24 hpi. It should be noted that the expression profiles of an immediate-early protein, ICP4, and an early protein, UL42, were almost the same between both cell lines, although the phosphorylation state of Sp1 was considerably different. Furthermore, as shown in Fig. 3B, in ATM-deficient AT10S/T-n cells from ataxia telangiectasia patients (43), Sp1 was originally present mostly as the faster-migrating form and only partially as the slower-migrating forms. The conversion efficiency from the faster-migrating form to slower-migrating forms was low in HSV-1-infected AT10S/T-n cells, as well as the case with ATM expression-silenced 293T cells. These observations strongly suggest that ATM is involved directly or indirectly in Sp1 hyperphosphorylation upon HSV-1 infection.

To further confirm the relationship between Sp1 hyperphosphorylation and ATM activation, the phosphorylation states of Sp1 were also compared in the human glioma cell lines M059J, which is DNA-dependent PK catalytic subunit (DNA-PKcs) null, and MJ-M6, which is a DNA-PKcs revertant of M059J cells transfected with the full-length DNA-PKcs cDNA expression vector (34) (Fig. 3C). It was previously shown that DNA-PKcs-deficient cells express very low levels of ATM and that recovery of DNA-PKcs partially restores ATM expression levels (25, 45). In MJ-M6 cells, the slower-migrating forms of Sp1 began to increase from 5 hpi, and almost all Sp1 proteins were converted to hyperphosphorylated forms by 10 hpi, appearing to correlate with expression levels of the activated ATM phosphorylated at Ser-1981. No change in the amount of ATM protein occurred throughout HSV-1 infection, whereas the levels of DNA-PKcs protein significantly decreased by 5 hpi. As previously reported, the degradation is dependent on the expression of the virus-encoded immediate-early protein ICP0,

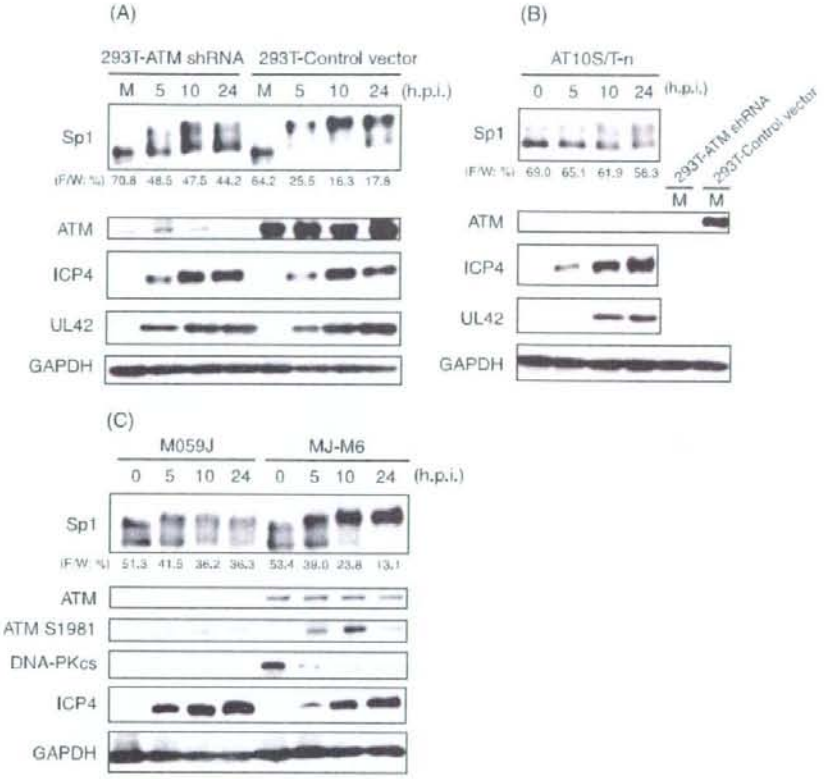

FIG. 3. ATM is involved in hyperphosphorylation of Sp1 induced by HSV-1 infection. (A and B) 293T-ATM shRNA and 293T-Control vector cells (A) and ATM defective AT10S/T-n cells (B) were infected with HSV-1 at an MOI of 10 and harvested at the indicated times postinfection. Whole-cell lysates were prepared, and equal amounts of proteins from each sample (7 to 15 μg) were subjected to immunoblot analysis with the indicated antibodies. Each value at the bottom of the panel of Sp1 ("F/W: %") represents the percentage of the level of the faster-migrating form to whole amounts of Sp1, calculated as described in Materials and Methods. M, mock infection. (C) Human glioma M059J (DNA-PKcs null and the lower level of ATM) and MJ-M6 (M059J cells expressing DNA-PKcs) cells were infected with HSV-1 at an MOI of 2.5 and harvested at the indicated times postinfection. Whole-cell lysates (15 μg) were subjected to immunoblot analysis for expression profiles of Sp1, ATM, ATM phosphorylated at Ser-1981, DNA-PKcs, ICP4, and GAPDH. Anti-GAPDH antibody was used to confirm equal protein loading.

viral ubiquitin ligase (35, 44). In contrast, in DNA-PKcs-defective M059J cells, the slower-migrating form of Sp1 appeared from 5 hpi and subsequently did not increase. Although the ATM phosphorylated at Ser-1981 increased slowly with progression of HSV-1 infection, the expression level was very low, reflecting the phosphorylation status of Sp1 in M059J cells. The expression profile of ICP4 was almost the same in both M059J and MJ-M6 cells. Overall, the results strongly suggest that activated ATM is involved directly or indirectly in the hyperphosphorylation of Sp1 in response to HSV-1 infection.

After IR, Sp1 is hyperphosphorylated dependent on activated ATM. In order to determine whether activation of ATM induces hyperphosphorylation of Sp1, HFF2 cells were exposed to 10 Gy of gamma irradiation, which generates double-strand DNA breaks, leading to activation of ATM-dependent DNA damage signal transduction. As shown in Fig. 4A, Sp1 was hyperphosphorylated immediately after IR accompanied by phosphorylation of Ser-1981 of ATM, leading to catalytic activation of the protein.

To determine whether IR-induced Sp1 phosphorylation depends on activated ATM, ATM-silenced 293T cells (293T-ATM shRNA) and 293T-Control vector cells were exposed to gamma irradiation (20 Gy) (Fig. 4B). In 293T-Control vector cells, IR induced the phosphorylation of ATM at Ser-1981 by 15 min post-IR, and simultaneously more than half of the Sp1 proteins were converted to hyperphosphorylated and slower-migrating forms. In contrast, in IR-treated ATM expression-silenced 293T cells, the phosphorylation status of Sp1 was almost unchanged. These observations with IR support the idea that the hyperphosphorylation of Sp1 is directly or indirectly dependent on activated ATM.

Mapping of Sp1 phosphorylation sites induced upon HSV-1 infection. Related PI-3-like kinases family members, ATM, DNA-PK, and ATR (ATM-Rad3-related), display kinase activity against serine (S) and threonine (T), followed by glutamine (Q) (SQ or TQ), residues (1, 6, 12, 13). Sp1 possesses 11 SQ sites and four TQ sites (Fig. 5A). With the aim of determination of the phosphorylation site(s), we constructed

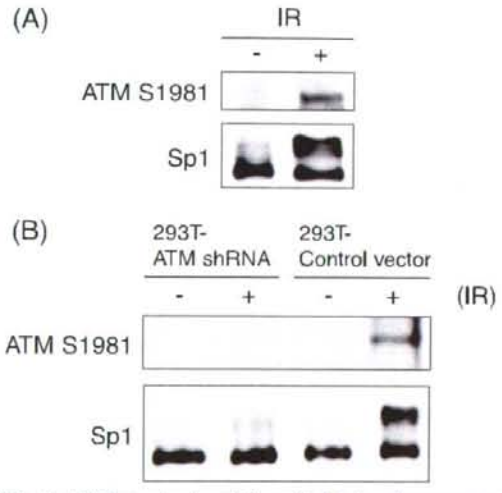

FIG. 4. (A) Hyperphosphorylation of Sp1 induced upon exposure to IR. HFF2 cells were exposed to gamma irradiation (IR) with 10 Gy and harvested at 15 min post-IR. Whole-cell lysates were prepared, and 30-μg aliquots of proteins from each sample were subjected to immunoblot analysis with anti-Sp1 and ATM S1981 antibodies. (B) Sp1 hyperphosphorylation induced upon IR is correlated with the activation of ATM. The 293T-ATM shRNA and 293T-Control vector cells were exposed to IR with 20 Gy and harvested at 15 min post-IR. Whole-cell lysates were prepared, and equal amounts of proteins from each sample were subjected to immunoblot analysis with anti-Sp1 and ATM S1981 antibodies. −, No IR.

expression vectors of Flag-tagged Sp1 (Flag-Sp1) containing alanine mutations of serine/threonine in each SQ/TQ site and investigated their phosphorylation in HSV-1-infected cells. As shown in Fig. 5B, most of the exogenously expressed Flag-tagged wild-type Sp1, like endogenous Sp1, was converted to slower-migrating forms upon HSV-1 infection, although a part of the recombinant protein (25 to 36%) remained as the faster-migrating form at 24 hpi. Phosphorylation patterns of Sp1 containing alanine mutations of Ser-36, Ser-81, Ser-85, Thr-98, Thr-250, Ser-281, Ser-291, Ser-296, Ser-313, Ser-351, Thr-394, Thr-427, and Ser-431 were almost the same as that of wild-type Sp1. The percentages of the remaining faster-migrating form to the total amounts of those mutated Sp1 were almost the same as or less than that of wild-type Sp1 (Fig. 5B, lower panel). In contrast, although Flag-Sp1 containing an alanine mutation of either Ser-56 or Ser-101 was also phosphorylated upon HSV-1 infection, the percentages of the faster-migrating form to total Sp1 were much higher (45 to 57%) compared to that seen with wild-type Sp1 (25%) (Fig. 5B, upper panel). Furthermore, Flag-Sp1 containing alanine mutations at both Ser-56 and Ser-101 resulted in considerably impaired conversion to the slower-migrating and hyperphosphorylated forms upon HSV-1 infection. Thus, mutation of Ser residues 56 and 101 individually or in tandem to alanine resulted in a reduction of the hyperphosphorylation of Sp1 upon HSV-1 infection.

Kim and DeLuca suggested that Sp1 is important for the expression of immediate-early and early genes whose promoters possess Sp1 binding sites and predicted that its hyperphosphorylation contributed to the downregulation of expression of these gene classes late in infection (31). However, the expression levels of ICP4 were almost constant among cells expressing wild-type Sp1 and a variety of mutated Sp1 proteins (Fig. 5B). Thus, even when the mutated Sp1 at Ser-56 and Ser-101 was expressed exogenously, we did not observe any reduced or overaccumulation of the immediate-early protein, ICP4, compared to exogenously expressed wild-type Sp1.

Ser-56 and Ser-101 on Sp1 become phosphorylated upon HSV-1 infection. In order to confirm that Sp1 is phosphorylated at Ser-56 and Ser-101 during HSV-1 infection, we prepared phosphopeptide-specific antibodies (α-Sp1 [pS56] and α-Sp1 [pS101] antibodies) raised against phosphorylated Ser-56 and Ser-101 residues, respectively, and characterized the specificity of each antibody (Fig. 6A and B). Exogenously expressed Sp1 proteins were immunoprecipitated with anti-Flag antibody from whole-cell lysates of HeLa cells that were transfected with each expression vector—pcDNA-RHF/Sp1, pcDNA-RHF/Sp1-S56A, or pcDNA-RHF/Sp1-S101A—followed by HSV-1 infection. Immunoprecipitated wild-type and mutant Sp1 samples were subjected to immunoblot analysis with the phosphopeptide-specific antibodies (Fig. 6A). α-Sp1 (pS56) could recognize wild-type Flag-Sp1 but not Flag-Sp1-S56A. Similarly, α-Sp1 (pS101) recognized wild-type Flag-Sp1 but not Flag-Sp1-S101A. In addition, both α-Sp1 (pS56) and α-Sp1 (pS101) showed CIAP-sensitive reactivity with endogenous Sp1 in whole-cell lysates obtained from HSV-1-infected HeLa cells at 12 hpi (Fig. 6B). Thus, it was proved that these two antibodies are directed against phospho-Ser-56 and phospho-Ser-101, respectively.

Next, we examined phosphorylation of Sp1 at Ser-56 and Ser-101 in HeLa cells and the ATM-deficient cell line, AT10S/T-n, throughout HSV-1 infection using the phosphopeptide-specific antibodies (Fig. 6C and D). In HeLa cells, phosphorylation of Sp1 at Ser-56 or Ser-101 was detected by 4 hpi and reached maximum level at 8 hpi. Similarly, the activated ATM phosphorylated at Ser-1981 was detected by 4 hpi and increased gradually. In contrast, in AT10S/T-n cells, both residues on Sp1 were not phosphorylated at all throughout infection. These observations clearly showed that both Ser-56 and Ser-101 residues on Sp1 become phosphorylated directly or indirectly by ATM in response to HSV-1 infection.

ATM phosphorylates Ser-101 but not Ser-56 on Sp1 in vitro. In order to investigate whether ATM can phosphorylate Sp1 directly, IP-kinase assays were performed (Fig. 7). Purified Sp1 from insect cells was subjected to an in vitro kinase assay with Flag-tagged wild-type ATM and kinase-dead ATM immunoprecipitated by anti-Flag antibody from cells transfected with each expression vector. Purified p53 known as a substrate for ATM (6) was used as a positive control. Equal amounts of Flag-tagged wild-type ATM and kinase-dead ATM were immunoprecipitated by anti-Flag antibodies. As shown in Fig. 7, Flag-tagged wild-type ATM phosphorylated Sp1 and p53 directly, whereas kinase-dead ATM did not. Thus, ATM can directly phosphorylate Sp1 in vitro.

Next, to determine whether ATM can phosphorylate Ser-56 and Ser-101 on Sp1 directly, GST fusion proteins of truncated Sp1 (8 to 167 amino acids) (GST-$Sp1_{8\text{-}167}$) and identical fragments with Ser-56 or Ser-101 or both mutated to alanine (GST-$Sp1_{8\text{-}167}$-S56A, GST-$Sp1_{8\text{-}167}$-S101A, and GST-$Sp1_{8\text{-}167}$-S56/101A) (Fig. 8A) were used as substrates in IP-kinase as-

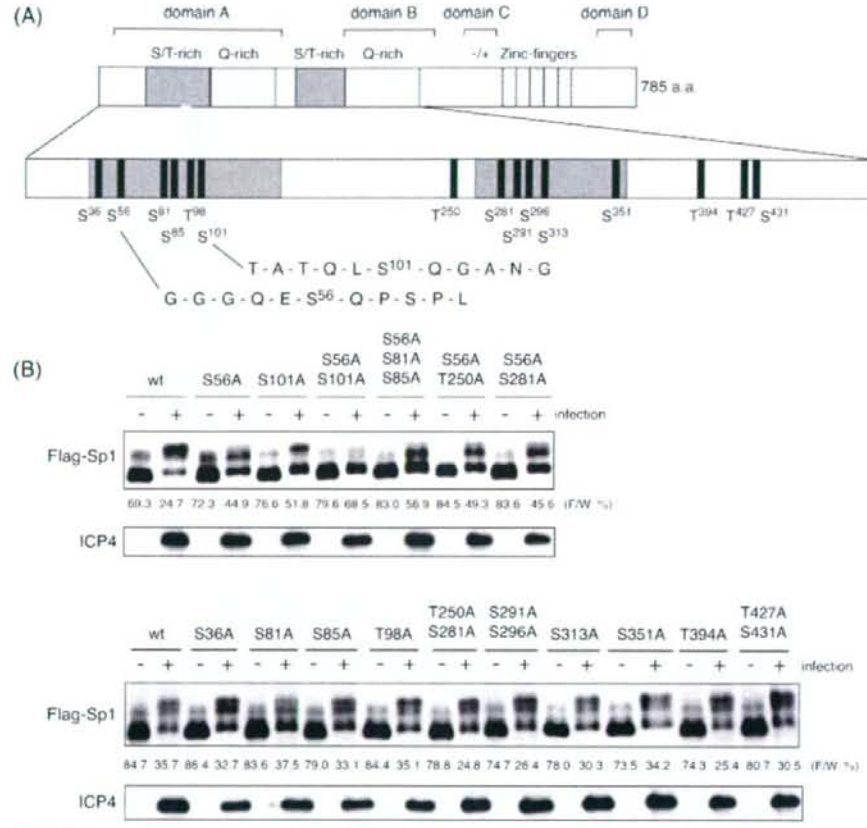

FIG. 5. Mapping of phosphorylation sites of Sp1 upon HSV-1 infection. (A) Schematic diagram of functional domains and putative ATM phosphorylation sites of Sp1. The 785 amino acids of Sp1 have two S/T-rich regions, two Q-rich regions, and three zinc fingers. The domains A, B, C, and D correspond to multiple transcriptional activation domains. The sign "−/+" represents a region of high charge density (14). Motifs of serine (S) or threonine (T), followed by glutamine (Q) (SQ and TQ) in Sp1, are putative phosphorylation sites for ATM. Sp1 contains 15 SQ and TQ sites. The amino acid sequences around Ser-56 and Ser-101 are shown in detail. (B) HeLa cells were transfected with pcDNA-RHF/Sp1 expressing wild-type (wt) Sp1 or a variety of expression vectors for mutated Sp1 containing the indicated serine or threonine residues replaced with alanine. Cells were infected with HSV-1 at an MOI of 10 at 24 h posttransfection and harvested at 24 hpi. Whole-cell lysates were prepared, and 25-μg portions of proteins from each sample were subjected to immunoblot analysis with anti-ICP4 antibody or anti-Flag antibody to detect exogenously expressed Sp1 proteins (Flag-Sp1). Each value at the bottom of the panel of Flag-Sp1 ("F/W: %") represents the percentage of level of the faster-migrating form to whole amounts of Flag-Sp1 as described in Materials and Methods.

says. The amounts of immunoprecipitated Flag-tagged wild-type ATM and kinase-dead ATM proved the same on immunoblot analysis (Fig. 8B). As shown in Fig. 8C, GST-$Sp1_{8-167}$-S56A, as well as wild-type GST-$Sp1_{8-167}$, was phosphorylated by wild-type ATM but not by kinase-dead ATM. In contrast, wild-type ATM could not phosphorylate GST-$Sp1_{8-167}$-S101A or GST-$Sp1_{8-167}$-S56/101A. These results clearly indicate that ATM can directly phosphorylate Sp1 at Ser-101 but not Ser-56. Considering this and the result that neither Ser-101 nor Ser-56 were phosphorylated upon HSV-1 infection in the ATM-defective cell line (Fig. 6D) together, other kinase(s) activated by ATM would phosphorylate Ser-56 on Sp1 upon HSV-1 infection.

ATM-dependent Sp1 phosphorylation does not affect Sp1-dependent transcriptional activity during viral infection. In order to examine whether ATM affects Sp1-dependent transcriptional activity upon HSV-1 infection, CAT activity from the Sp1 responsive promoter in ATM expression-silenced 293T cells (293T-ATM shRNA) was compared to those in ATM expression-intact 293T cells (293T-Control vector) (Fig. 9). Sp1 stimulates transcription from promoters containing a GC-rich recognition element, the GC-box (15, 16, 19), and is also important for the regulation of TATA-less genes that encode housekeeping proteins (23). As depicted in Fig. 9A, the CAT reporter plasmid, p65F1CAT, has a promoter sequence (−575 to +38) of p65, an NF-κB subunit, containing three GC-boxes upstream of the CAT gene without any TATA consensus sequence (62). 293T-ATM shRNA cells and 293T-Control vector cells transfected with p65F1CAT were infected with HSV-1 at 24 h posttransfection and harvested at 12 hpi. The lysates from

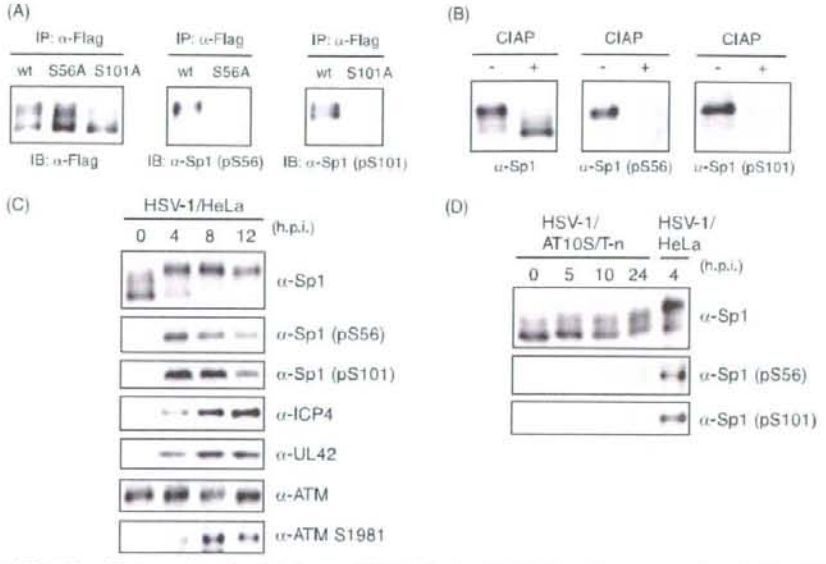

FIG. 6. Ser-56 and Ser-101 of Sp1 are phosphorylated upon HSV-1 infection. (A) HeLa cells were transfected with pcDNA-RHF/Sp1 (wt), pcDNA-RHF/Sp1-S56A, or pcDNA-RHF/Sp1-S101A and infected with HSV-1 at an MOI of 10 at 24 h posttransfection. At 24 hpi, cells were harvested and lysed. The whole-cell lysates were subjected to IP with anti-Flag M2 affinity resin, and the immunoprecipitated samples were subjected to immunoblot (IB) analysis with anti-Flag, α-Sp1 (pS56), and α-Sp1 (pS101) antibodies. (B) Whole-cell lysates obtained from HSV-1-infected HeLa cells at 12 hpi were treated with (+) or without (−) CIAP. The samples were applied for immunoblot analysis with the indicated antibodies. (C) HeLa cells were infected with HSV-1 at an MOI of 10 and harvested at the indicated times postinfection. Whole-cell lysates were prepared, and equal amounts of proteins from each sample were applied for immunoblot analysis with the indicated antibodies. (D) AT10S/T-n cells were infected with HSV-1 at an MOI of 10 and harvested at the indicated times postinfection. Whole-cell lysates were prepared and subjected to immunoblot analysis with the indicated antibodies. Whole-cell lysate from HSV-1-infected HeLa cells at 4 hpi was also applied as a positive control.

both cells were subjected to CAT assay, and the transcriptional activities were analyzed by calculating the percentage of the conversion of unacetylated [^{14}C]chloramphenicol to the acetylated form. In a CAT assay for p65F1CAT, the transcriptional activity from the Sp1 responsive promoter in 293T-ATM shRNA cells was almost the same (only a 1.2-fold increase) as that in 293T-Control vector cells (Fig. 9B and C). Next, another reporter plasmid, pCAT TATA+Sp1(−55)+Sp1(−75) (Fig. 9D) containing two GC-boxes and TATA consensus sequence of human cytomegalovirus (HMCV) major immediate-early gene upstream of the CAT gene (27) was used as TATA-dependent Sp1 responsive promoter. Similarly, the transcriptional activity from the promoter in 293T-ATM shRNA cells infected with HSV-1 was almost the same as that in 293T-Control vector cells (Fig. 9E and F). In 293T-Control vector cells Sp1 was detected mainly as the slower-migrating and hyperphosphorylated forms at 12 hpi. In contrast, in 293T-ATM shRNA cells, Sp1 was detected mostly as the faster-migrating form and partially as the slower-migrating form (Fig. 9C and F, inset images). Phosphorylation of Ser-56 and Ser-101 on Sp1 was observed in 293T-Control vector cells, while the phosphorylation was not in 293T-ATM shRNA cells (data not shown). As shown in Fig. 3A, the expression profiles of ICP4, whose promoter possesses several Sp1-binding sites, in 293T-ATM shRNA and 293T-Control vector cells were almost the same throughout HSV-1 infection, corresponding well with the same Sp1-dependent transcriptional activities in both cells obtained in the reporter-gene analyses of Fig. 9. Collectively, ATM-dependent Sp1 phosphorylation does not appear to affect the Sp1-dependent transcriptional activity during viral infection.

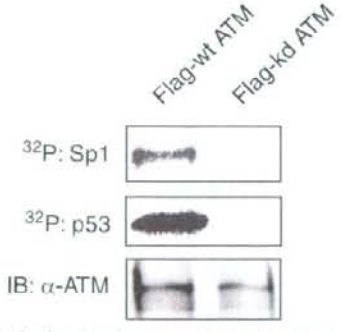

FIG. 7. Sp1 is phosphorylated by ATM in vitro. The lysates of 293T cells transfected with plasmid expressing Flag-tagged wild-type ATM (Flag-wt ATM) or kinase-dead ATM (Flag-kd ATM) were immunoprecipitated with anti-Flag antibody. Each of immunocomplexes containing Flag-wt ATM or Flag-kd ATM protein were incubated with purified Sp1 or p53 as substrates in the presence of [γ-^{32}P]ATP. Sp1 and p53 were resolved by SDS–10% PAGE, followed by autoradiography. The amounts of immunoprecipitated Flag-wt ATM and Flag-kd ATM were confirmed by immunoblot analysis with anti-ATM antibody.

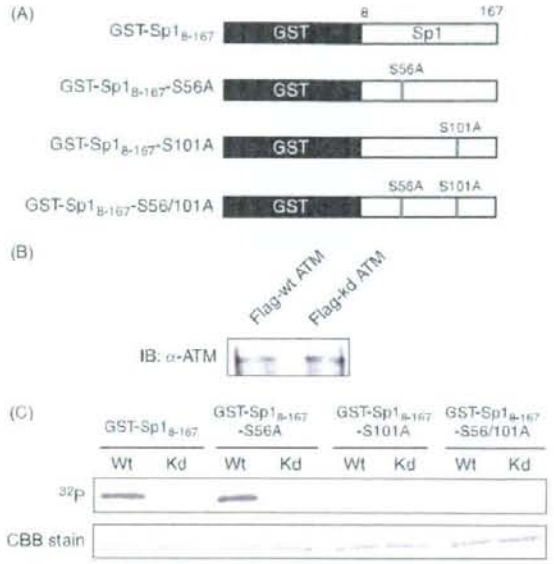

FIG. 8. ATM phosphorylates Sp1 at Ser-101 but not Ser-56 in vitro. (A) Schematic diagram of GST fusion proteins of truncated Sp1 and identical fragments with one or both of Ser-56 and Ser-101 mutated to alanine. (B) Lysates of 293T cells transfected with plasmid expressing Flag-tagged wild-type ATM (Flag-wt ATM) or kinase-dead ATM (Flag-kd ATM) were immunoprecipitated with anti-Flag antibody. Immunocomplexes of Flag-wt ATM or Flag-kd ATM were resolved on SDS–10% PAGE gel and subjected to immunoblot analysis with anti-ATM antibody. (C) IP-kinase assays. GST-$Sp1_{8-167}$, GST-$Sp1_{8-167}$-S56A, GST-$Sp1_{8-167}$-S101A, and GST-$Sp1_{8-167}$-S56/101A were expressed in *E. coli*, purified, and used as substrates for IP-kinase assays. Immunocomplexes containing Flag-wt ATM (Wt) or Flag-kd ATM (Kd) protein were each incubated with purified GST-$Sp1_{8-167}$, GST-$Sp1_{8-167}$-S56A, GST-$Sp1_{8-167}$-S101A, or GST-$Sp1_{8-167}$-S56/101A as substrates in the presence of [γ-^{32}P]ATP. Samples were resolved by SDS–10% PAGE, followed by autoradiography. The amounts of each GST fusion protein were confirmed by Coomassie brilliant blue (CBB) staining.

DISCUSSION

It was found here that hyperphosphorylation of the transcription factor Sp1 upon HSV-1 infection is mainly due to ATM and/or cellular kinase(s) activated by ATM rather than individual HSV-1 encoded PKs. Hyperphosphorylation of Sp1 upon HSV-1 infection was thus impaired in ATM-deficient or -expression silenced cells. Although at least two sites of Ser-56 and Ser-101 could be phosphorylated upon HSV-1 infection, ATM was here found to directly phosphorylate Sp1 at Ser-101 but not at Ser-56. To our knowledge, this is a first report describing determination of the target site on Sp1 for ATM. Involvement of ATM in Sp1 phosphorylation is also supported by the previous reports that Sp1 and ATM coimmunoprecipitate reciprocally in vivo and that Sp1 directly interacts with the kinase region of ATM in vitro (21).

Hyperphosphorylation of Sp1 is observed also in infection of other herpesviruses such as HCMV and Epstein-Barr virus (EBV). HCMV infection results in increased phosphorylated forms of Sp1, together with an increased level of Sp1 (27, 62), and the ATM DNA damage checkpoint pathway is activated in response to HCMV infection (18, 38). Also, induction of lytic replication in EBV latently infected cells results in hyperphosphorylation of Sp1 (S. Iwahori, A. Kudoh, and T. Tsurumi, unpublished result) and EBV lytic replication elicits ATM checkpoint signal transduction (33). Thus, ATM-dependent Sp1 hyperphosphorylation might be a common phenomenon during the lytic replication of herpesviruses.

Although phosphorylation of Sp1 at Ser-56 was not detected at all upon infection in ATM-deficient cells, ATM by itself could not phosphorylate Ser-56 on Sp1 in vitro, suggesting that other cellular kinase(s) activated by ATM could be involved in the Ser-56 phosphorylation. The sequence of Ser-56 followed by glutamine is known as putative phosphorylation site for related members of the PI-3-like kinase family such as ATM, ATR, and DNA-PK. Chen et al. have recently suggested that ATM is likely the kinase mediating IR-induced DNA-PKcs phosphorylation required for full activation of DNA-PKcs (7). Sp1 phosphorylation by DNA-PK has already been reported from studies of human immunodeficiency virus type 1 infection (11). However, as shown in Fig. 3C, the level of DNA-PKcs decreases significantly at early stages of HSV-1 infection, the degradation being in a virus-encoded ICP0-dependent manner as reported by others (35, 44). Also, activation of ATR is minimal during HSV-1 infection (37, 53), although the ATR PK activity is dependent upon ATM (29, 42, 58). Furthermore, it has recently been reported that HSV-1 disrupts the ATR-dependent DNA damage response through destruction of the usually tight colocalization of ATR and ATRIP (59). Thus, involvement of ATR and DNA-PK in phosphorylation of Ser-56 on Sp1 upon HSV-1 infection is unlikely. In response to IR, ATM phosphorylates and activates checkpoint kinases, Chk1 and Chk2, that play roles as signal transducers (3). We reported that the activation of Chk1 and Chk2 was induced upon HSV-1 infection (53). However, since the sequence around Ser-56 is distinct from Chk1 and Chk2 target motif (Arg-x-x-Ser) (8, 55), it is also unlikely that activated Chk1 and Chk2 are involved in the phosphorylation of Sp1 at Ser-56.

With respect to the role of Sp1 hyperphosphorylation during HSV-1 infection, Kim and DeLuca have reported purified Sp1 from HSV-1-infected cells at 12 hpi to exhibit reduced transcriptional activity in an in vitro transcription assay, although the DNA-binding activity of Sp1 was unchanged until 8 hpi (31). These researchers suggested that the reduced transcriptional activity of Sp1 may be due to the hyperphosphorylation of Sp1 and contribute to the reduced transcription of immediate-early and early genes with Sp1-binding sites in its promoters at late stages of infection (31). We also observed the reduced Sp1-dependent transcriptional activity upon HSV-1 infection in reporter gene assay (data not shown). As shown in Fig. 9, however, the transcriptional activity from the Sp1 responsive promoter in 293T-ATM shRNA cells upon HSV-1 infection was almost the same as that in 293T-Control vector cells. In addition, there was almost no difference between the expression profile of ICP4, whose promoter possesses several Sp1-binding sites, in 293T-ATM shRNA and that in 293T-Control vector cells throughout HSV-1 infection, although Sp1 hyperphosphorylation was impaired in 293T-ATM shRNA cells (Fig. 3A), a finding corresponding well with our previous report that there is no difference in the yields of HSV type 2 in